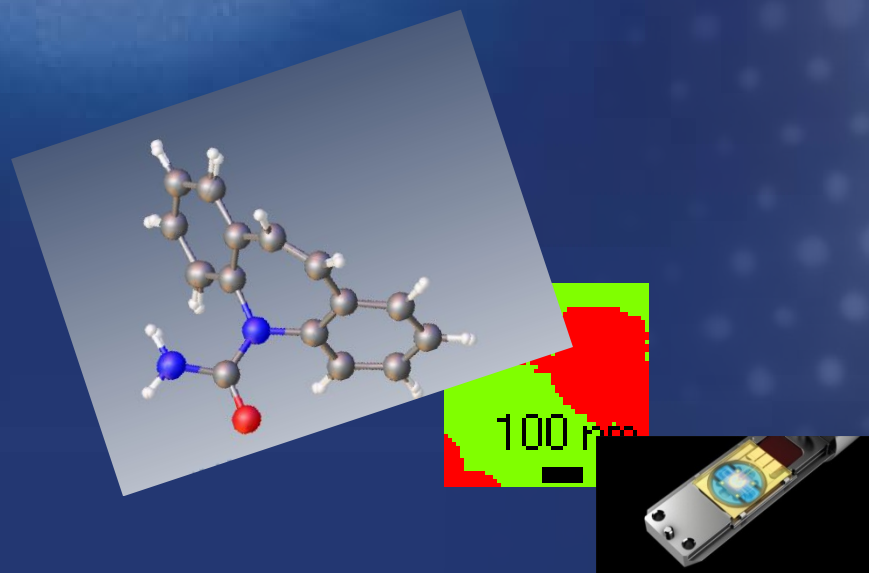
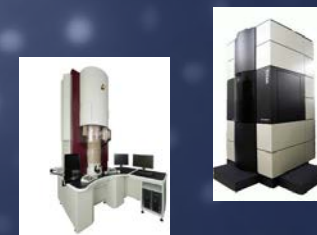


In situ materials characterization with 4D STEM scanning precession diffraction using novel pixelated detectors



Dr. Stavros Nicolopoulos
Director NanoMEGAS



GN
MEBA



**GROUPEMENT NATIONAL DE
MICROSCOPIE ELECTRONIQUE A BALAYAGE
ET DE MICROANALYSES**



En convention de coopération avec la Société Française de Physique

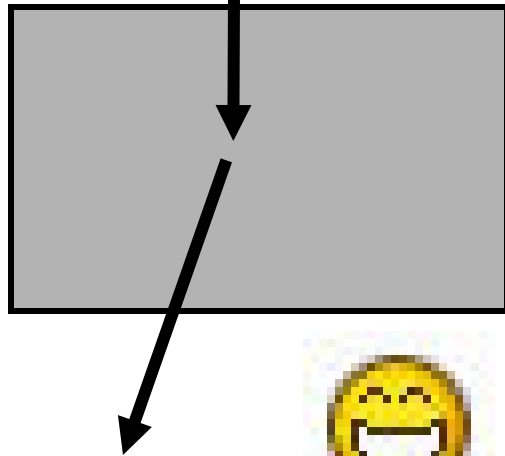


BRUSSELS RESEARCH & DEVELOPMENT FACILITY

Electron diffraction : Dynamical effects

Weak interaction

Incoming radiation

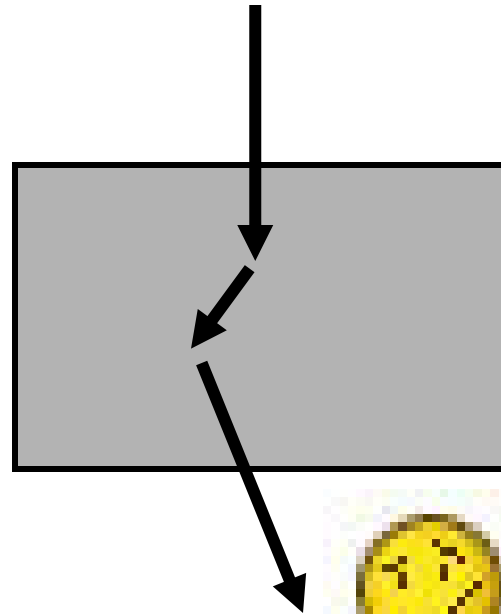


Kinematical scattering
Single scattering

$$I_{hkl} \sim (F_{hkl})^2$$

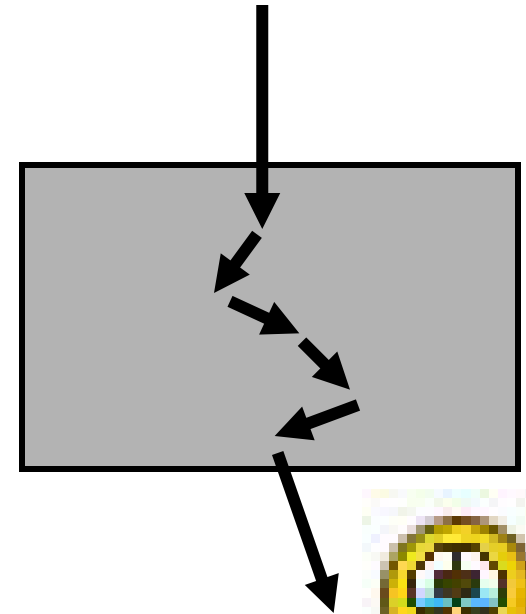
Always the case for X-ray

Strong interaction



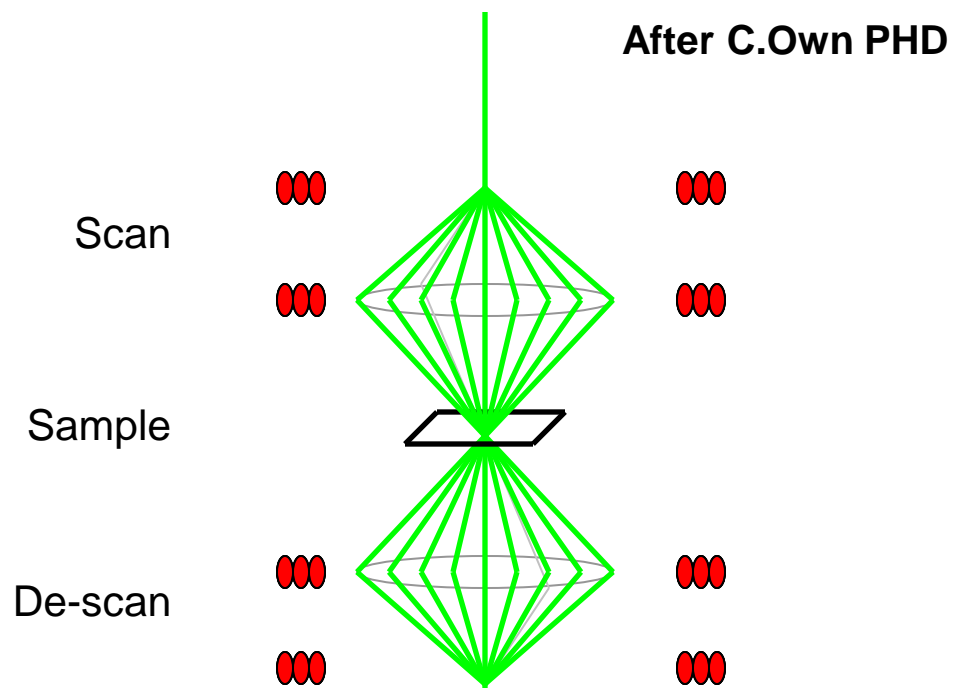
Dynamical scattering
2-beam scattering
Blackman formula

$$I_{hkl} \sim F_{hkl}$$



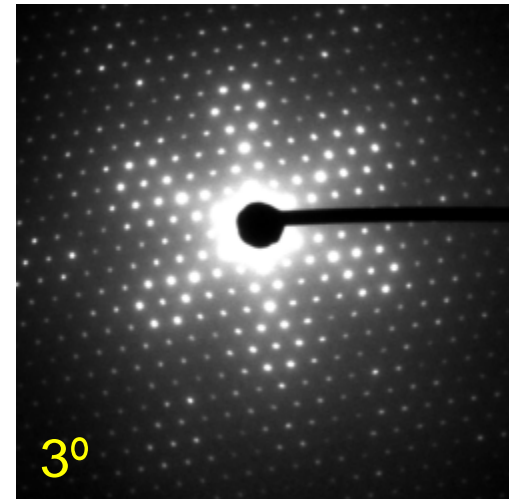
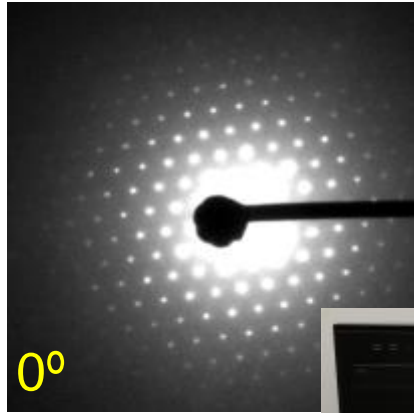
Dynamical scattering
Multi-beam?

Vincent-Midgley Precession Method



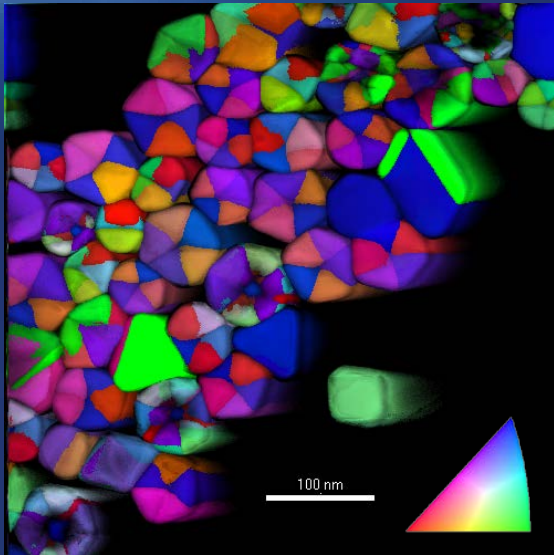
Non-precessed

Precessed



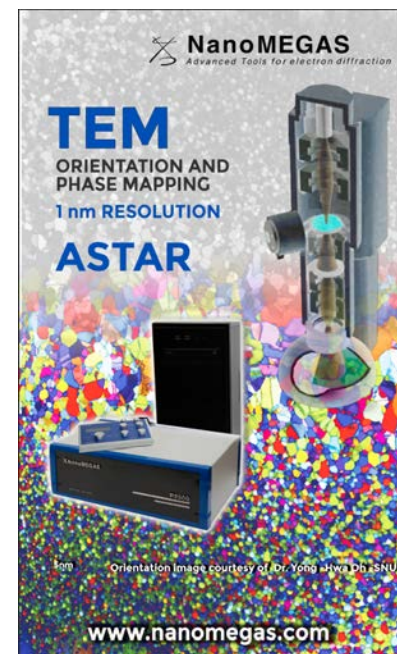
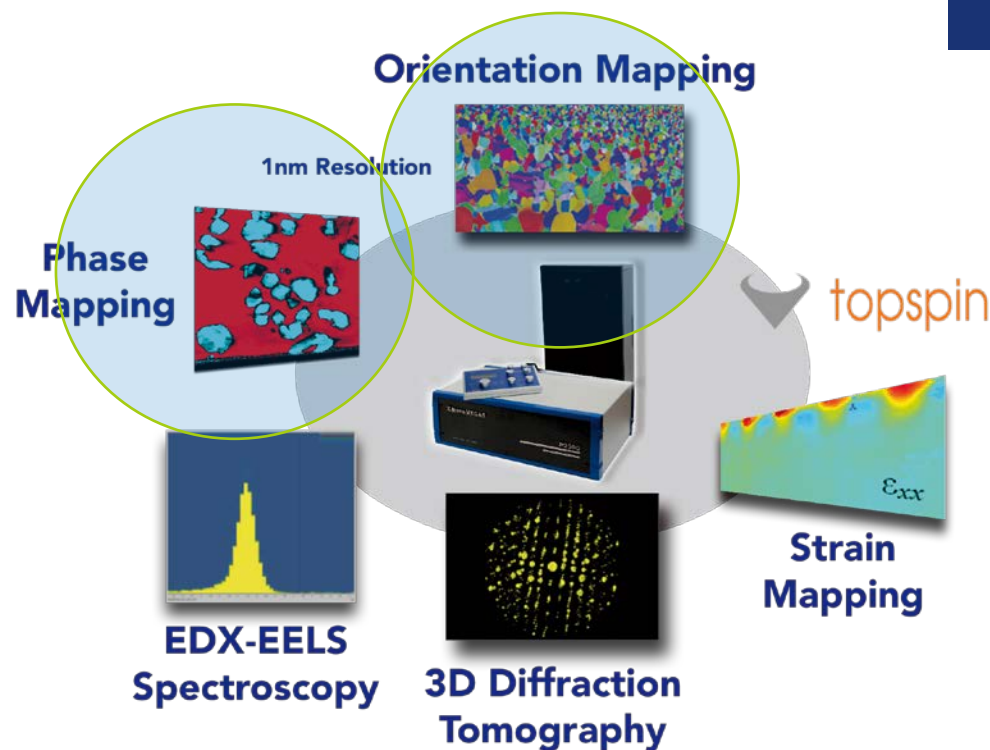
Precession unit Digistar
more kinematical ED intensities

ASTAR : orientation & phase mapping



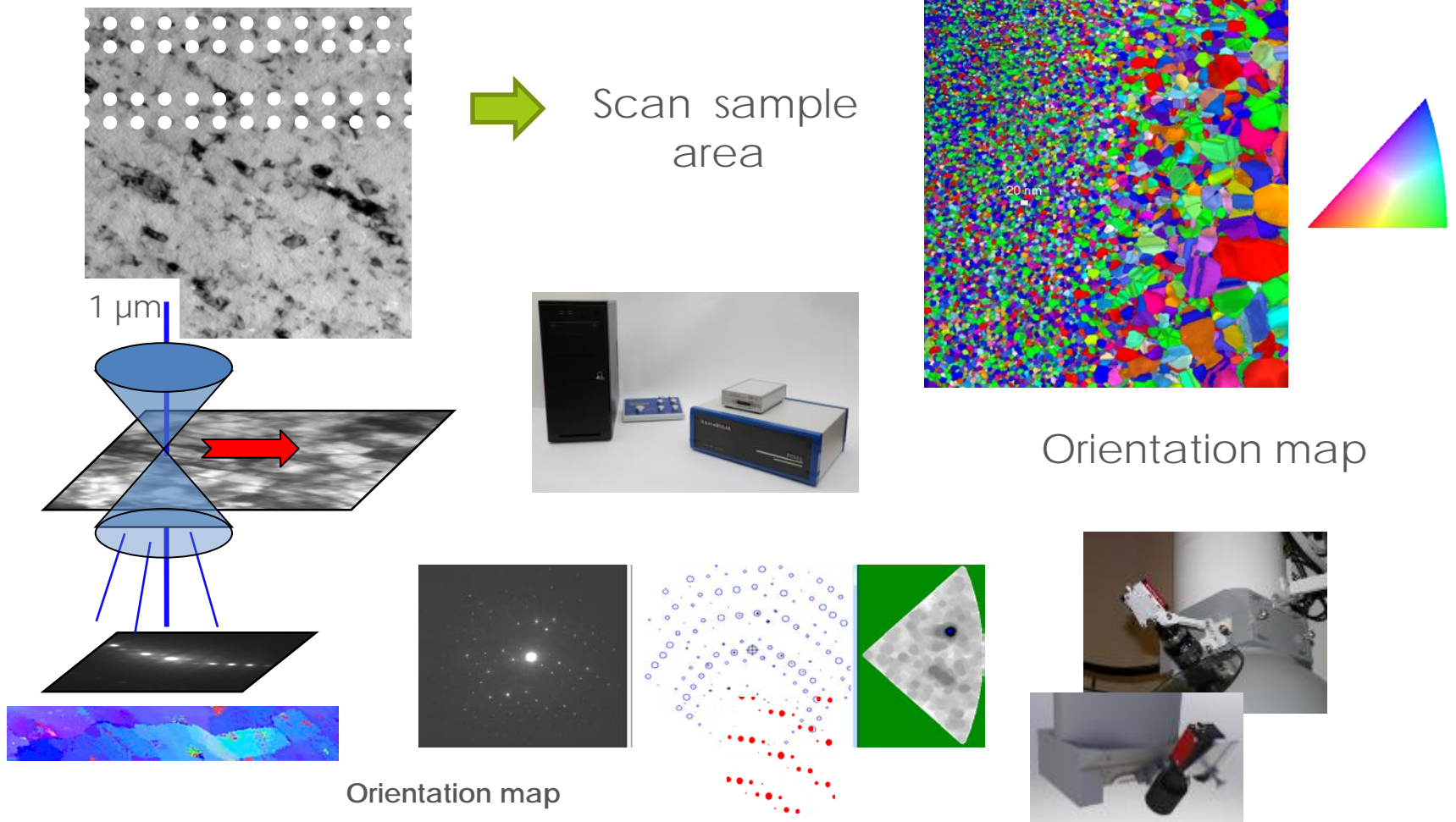
ASTAR: TEM Orientation and Phase Mapping

➤ 180 installations world-wide in TEM



ASTAR : EBSD type tool for TEM

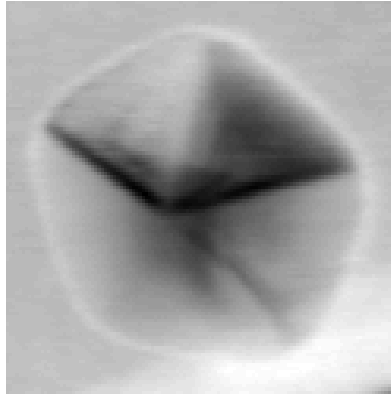
ASTAR : Automated Crystal Orientation Mapping



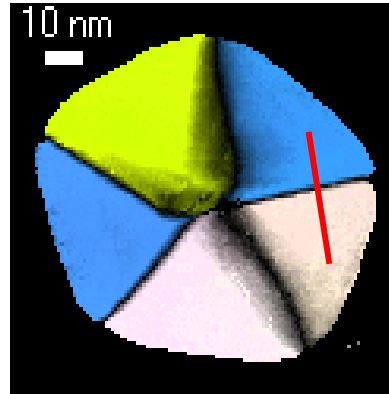
ASTAR : EBSD type tool for TEM

ASTAR : 1 nm spatial resolution orientation map

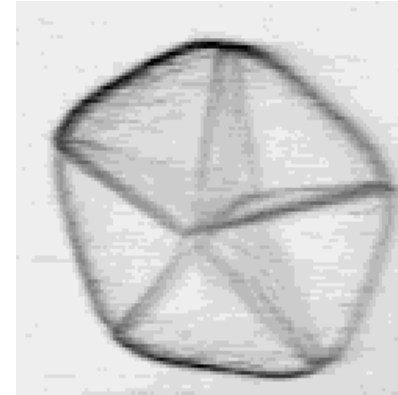
Multi-twinned gold particles (JEOL ARM 200)



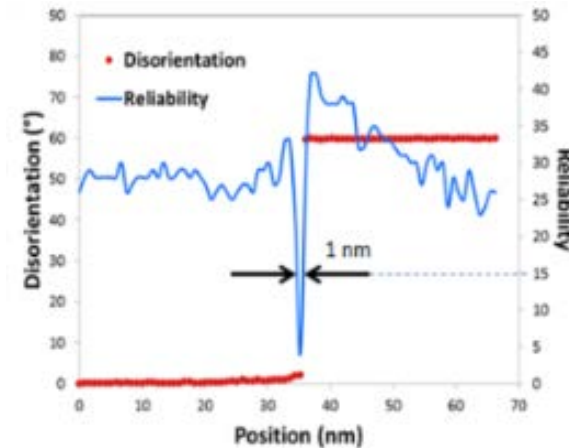
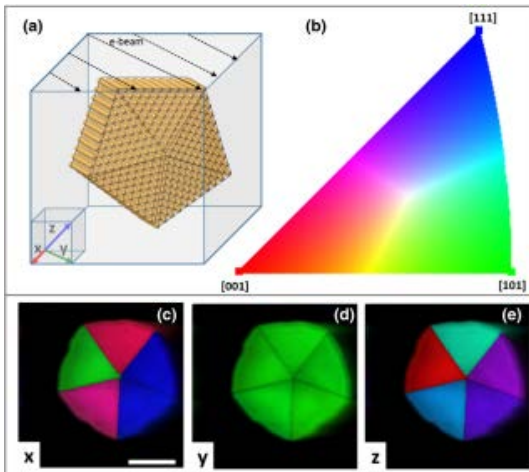
Virtual Bright-Field



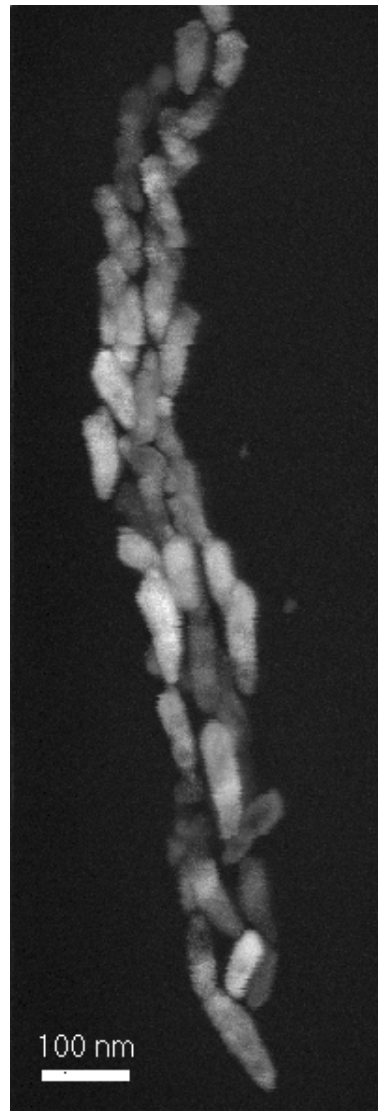
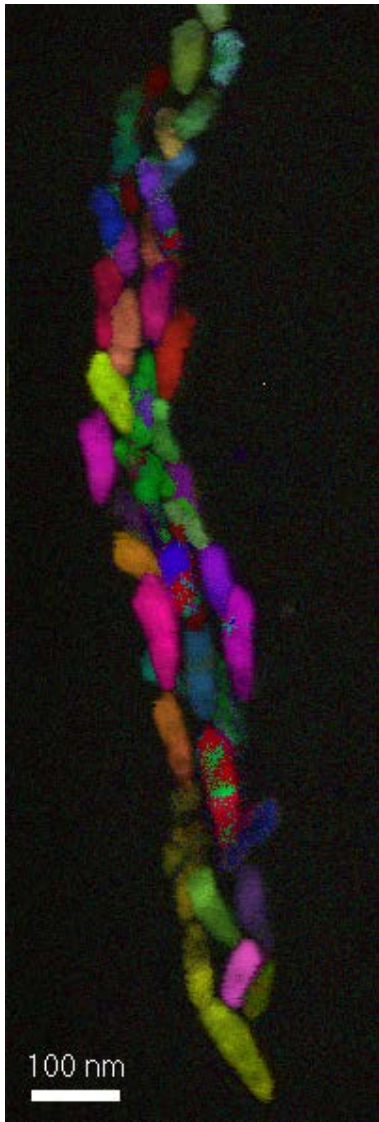
Orientation + Reliability



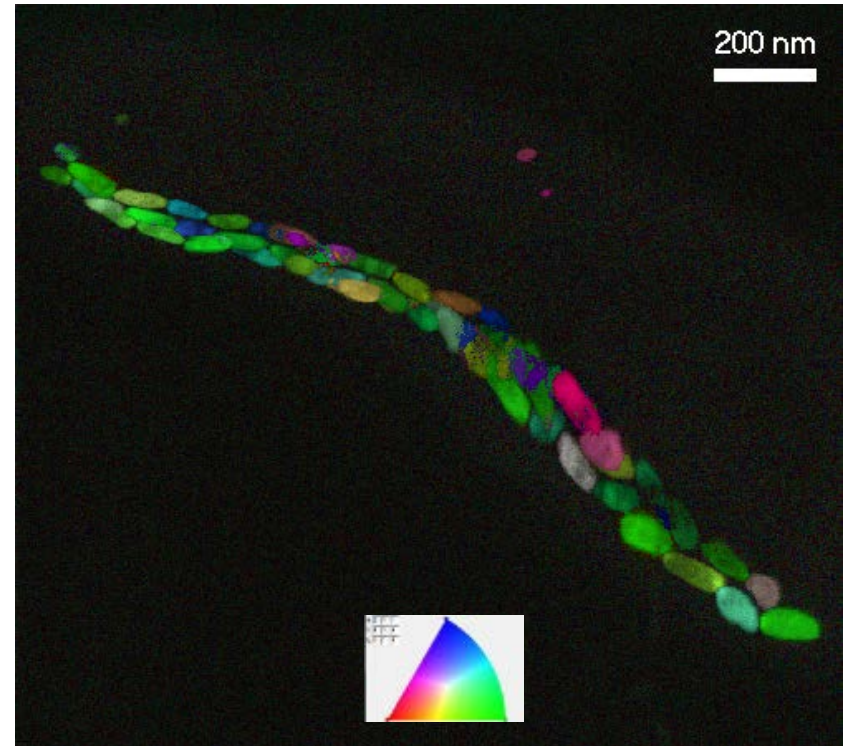
DP cross-correlation



ASTAR : EBSD type tool for TEM



ASTAR orientation map



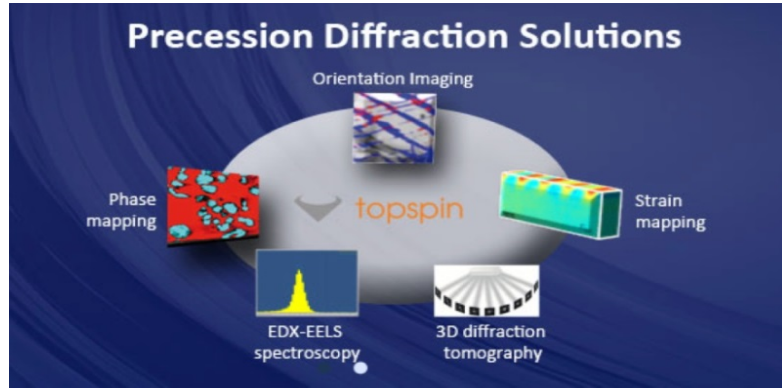
Data, courtesy Dr. J. Bourgon CNRS Thiais

Magnetite nanocrystals and magnetotactic BACTERIA

NanoMEGAS - TEM Cs corr / high end microscopes



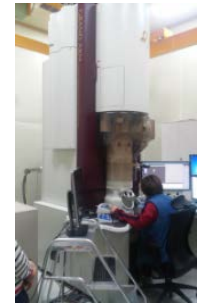
TITAN HIGH Base



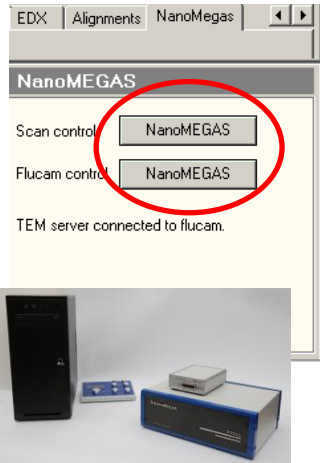
> 400 PED related articles in 12 years
> 180 installations worldwide



ARM 200 FEG Double Cs



ARM 300 Double Cs



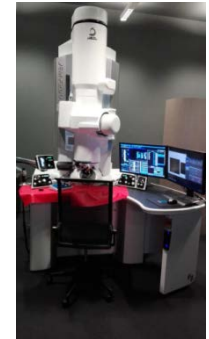
TITAN LOW Base



TALOS



HF5000



F200

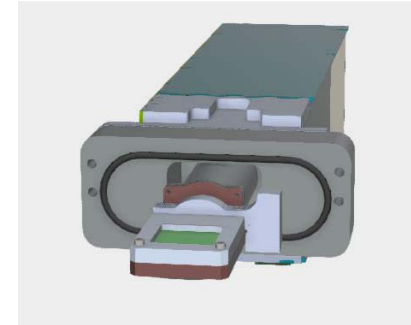
ASTAR and PIXELATED DETECTORS



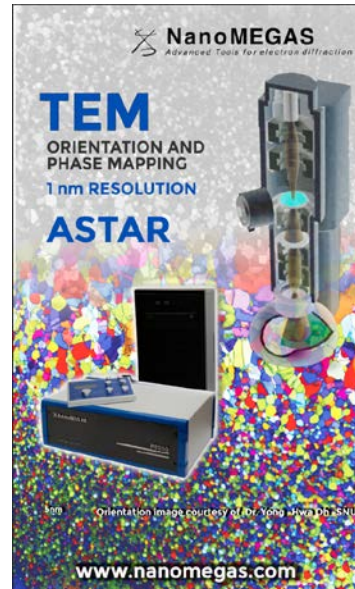
 **Quantum**
DETECTORS



AMSTERDAM
SCIENTIFIC
INSTRUMENTS



 **GATAN**



OneView

 **GATAN**

**ASTAR compatible with
Direct Detection cameras**



DECTRIS
detecting the future

ASTAR and PIXELATED DETECTORS

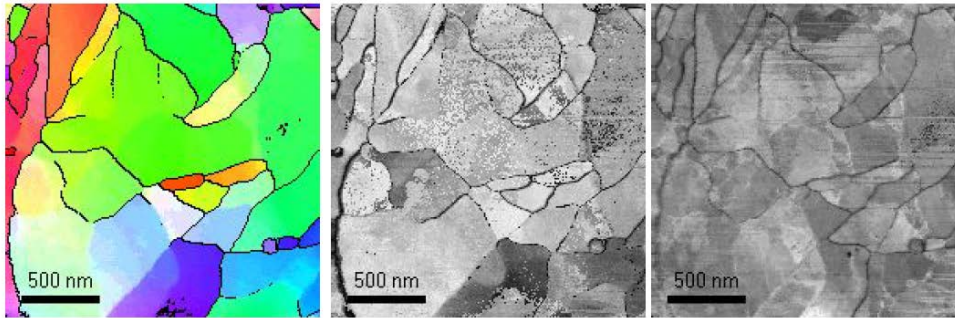


Fig. 1 Orientation mapping results from diffraction patterns acquired with Dectris camera. From left to right: Color coded orientation map with grain boundaries, orientation reliability map and index map

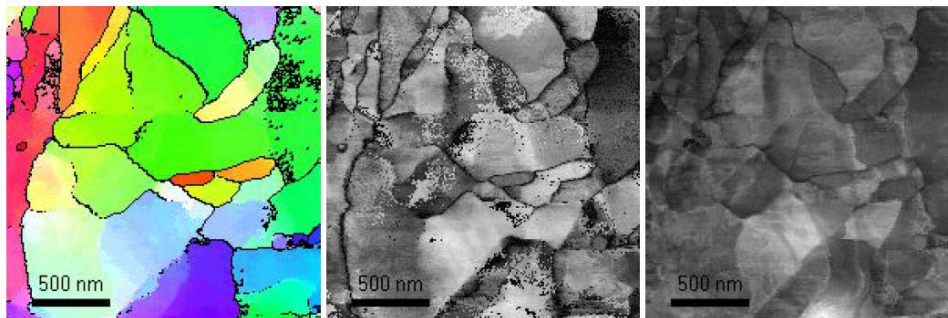


Fig. 2 Orientation mapping results from diffraction patterns acquired with Stingray camera. From left to right: Color coded orientation map with grain boundaries, orientation reliability map and index map

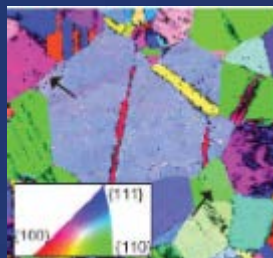


ASTAR orientation / phase mapping : in *SITU* and correlative microscopy

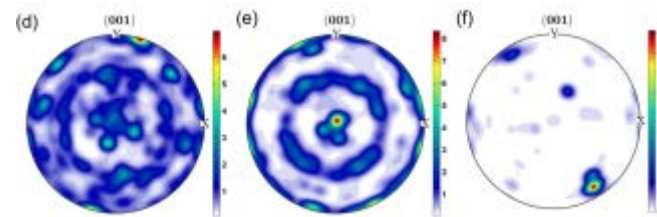
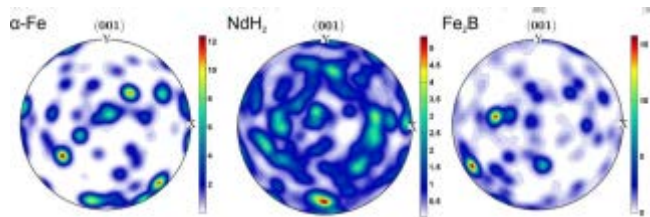
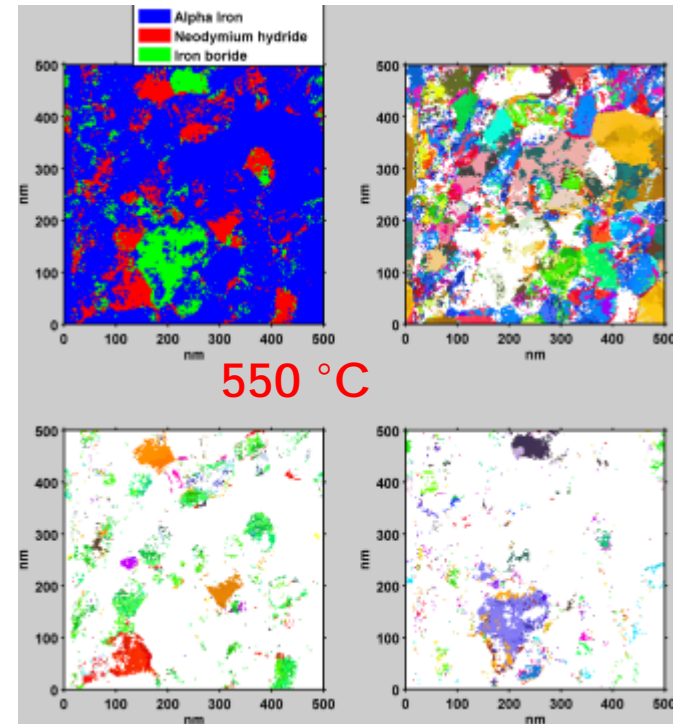
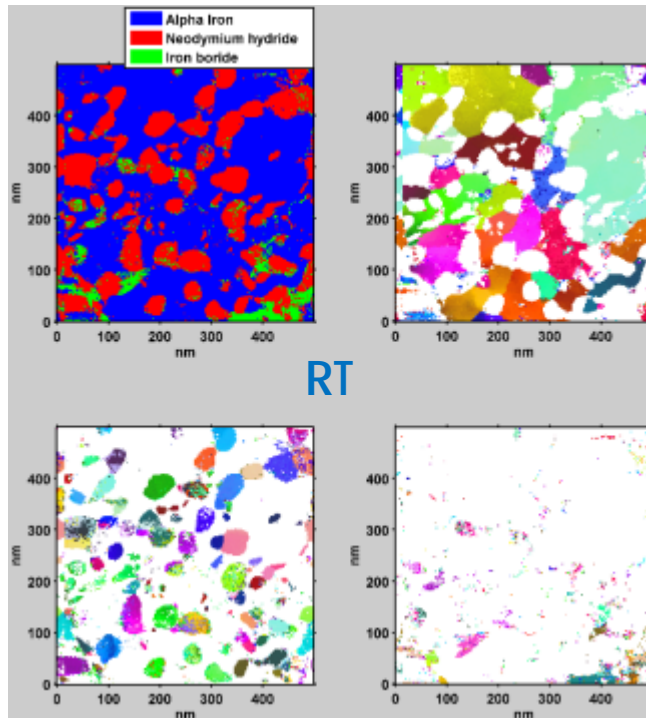
0 % strain



6.5 % strain



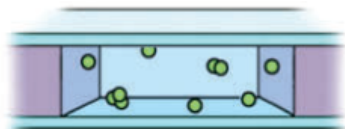
ASTAR - in situ texture analysis and HEATING of Nd-Fe-B powder particles



In situ LC- TEM : the Nano-aquarium

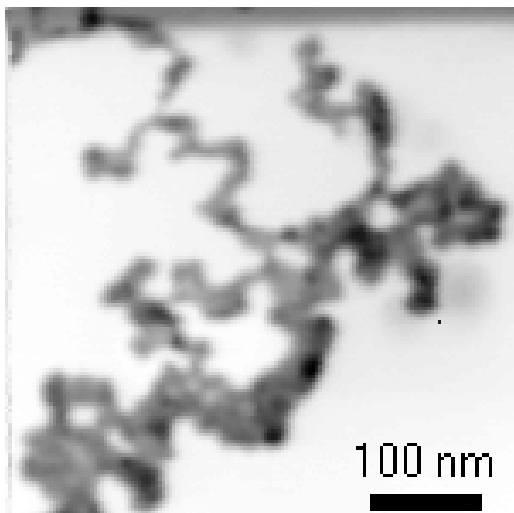


Collaboration with
Dr. A.Demortiere
Univ Picardie France

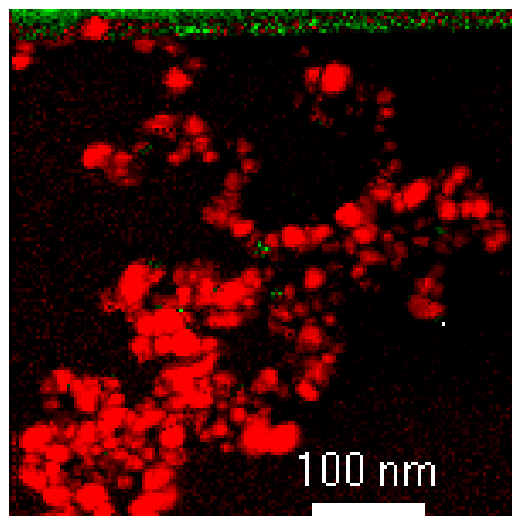


The loaded liquid sample is sealed and imaged using TEM in the native liquid environment.

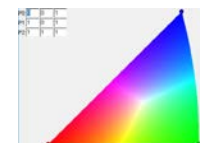
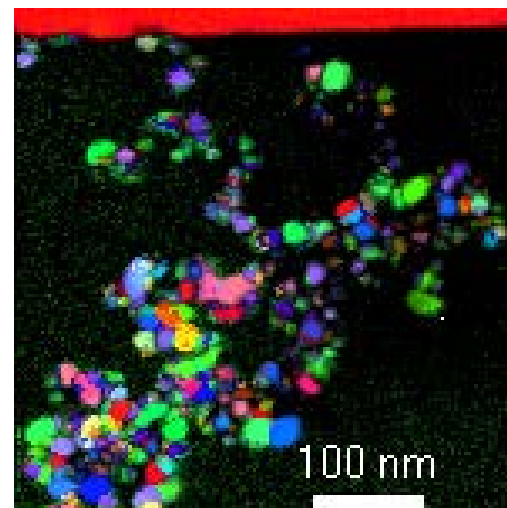




ASTAR Virtual brightfield

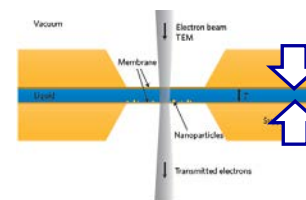


ASTAR Phase Map with index quality and phase reliability



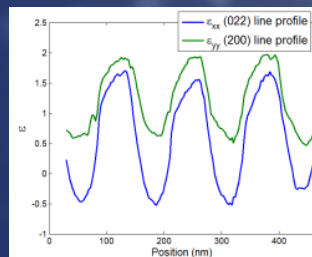
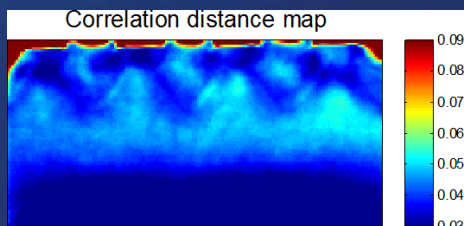
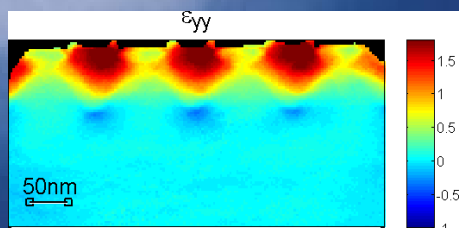
(a) TEM bright field image of gold nanoparticles in water, (b) ASTAR phase mapping where shows all pixels are gold and (c) ASTAR orientation map, different colors represent different orientations shown in the stereographic projection. (Coutesy Dr. Muriel Veron CNRS Grenoble France)

New frontier

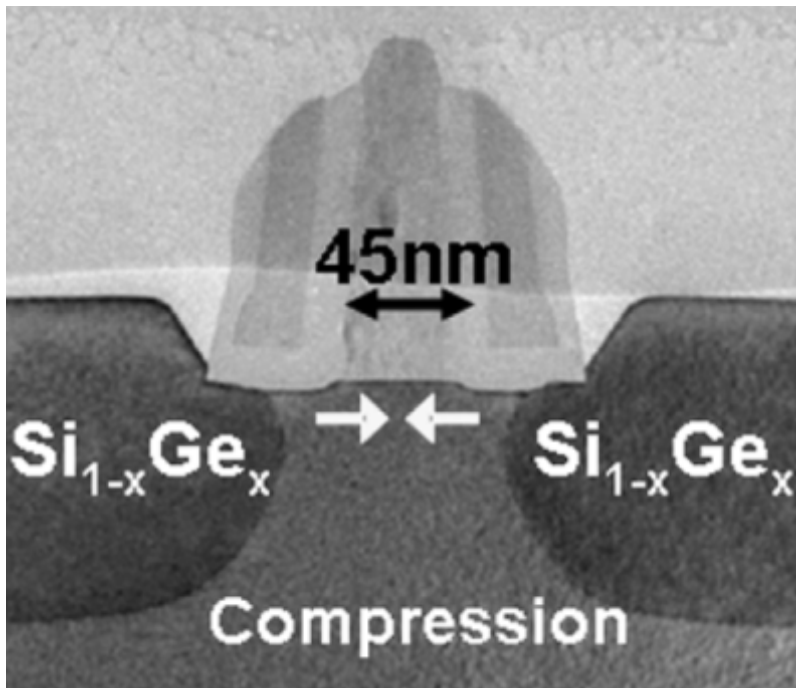


LC spacer
150 nm

Strain mapping at nm scale

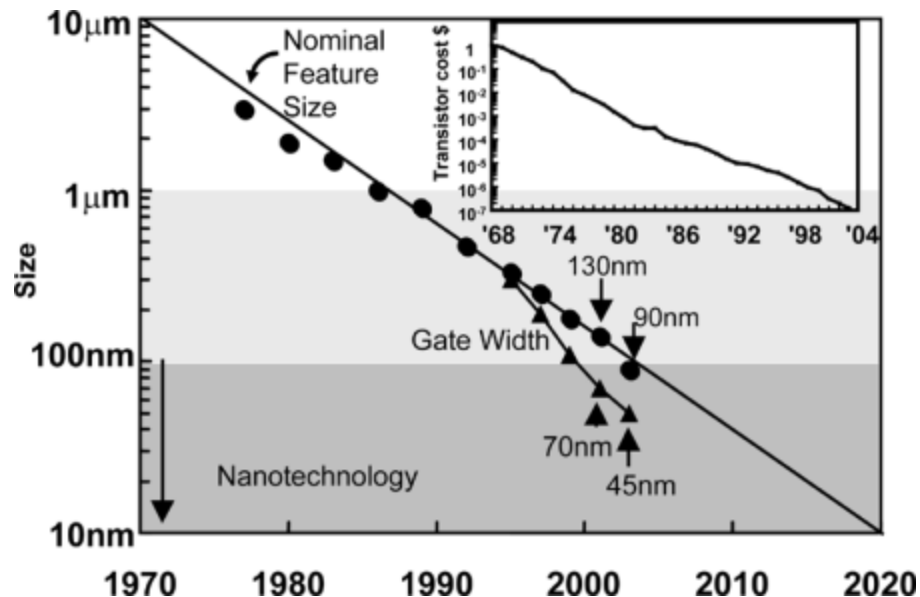


STRAIN ON SEMICONDUCTOR DEVICES



pMOSFET

Thompson et al., IEEE Trans. On Electron Devices, VOL. 51, NO. 11, 2004



Industry Requirements

- Desired spatial resolution ~ 1 nm
- Strain sensitivity $\ll 0.1\%$
- Highly automated

Conventional Nano-Beam Diffraction

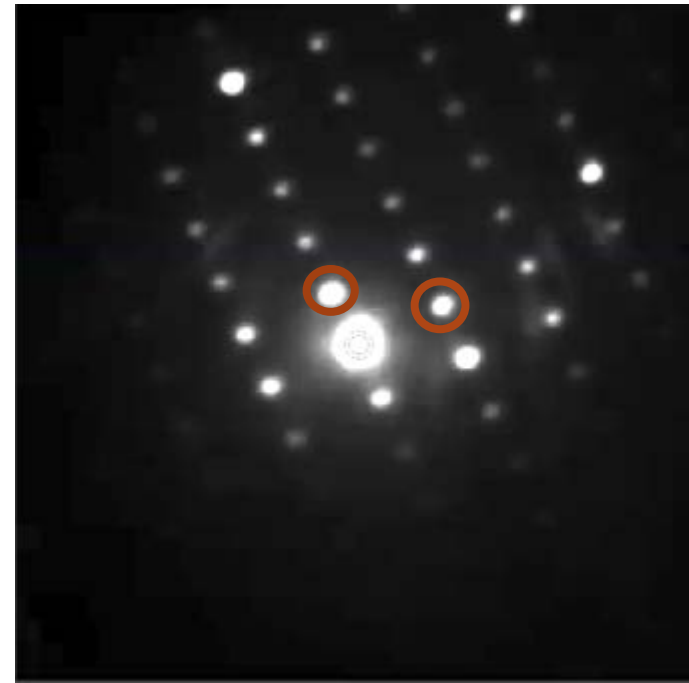
Strain determined by measuring shift in spot positions

Advantage

- High spatial resolution - better than 1 nm

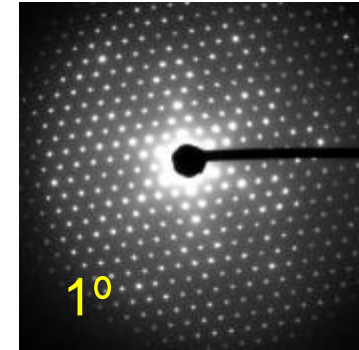
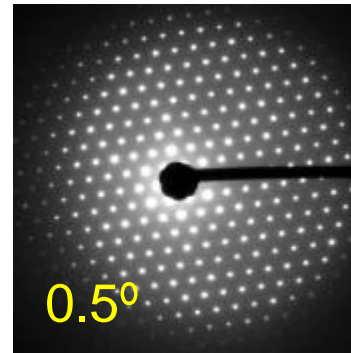
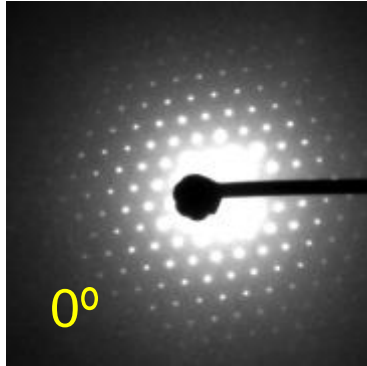
Disadvantage

- Dynamical diffraction -- thickness related effects

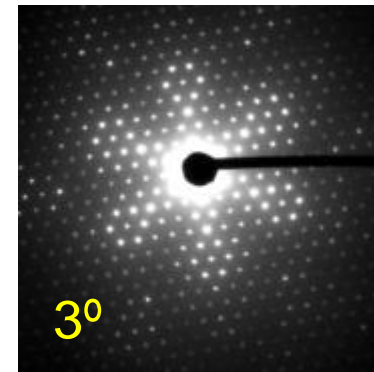
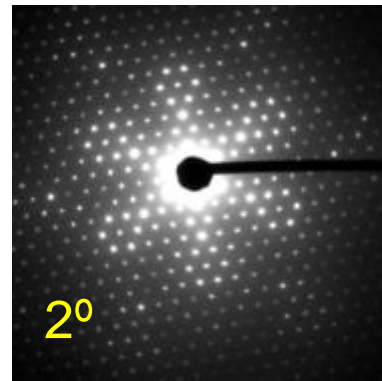


D Cooper et al., Journal of Physics: Conference Series **326** 012025 (2011).

Strain Measurement via NBD with Precession & Automated Analysis



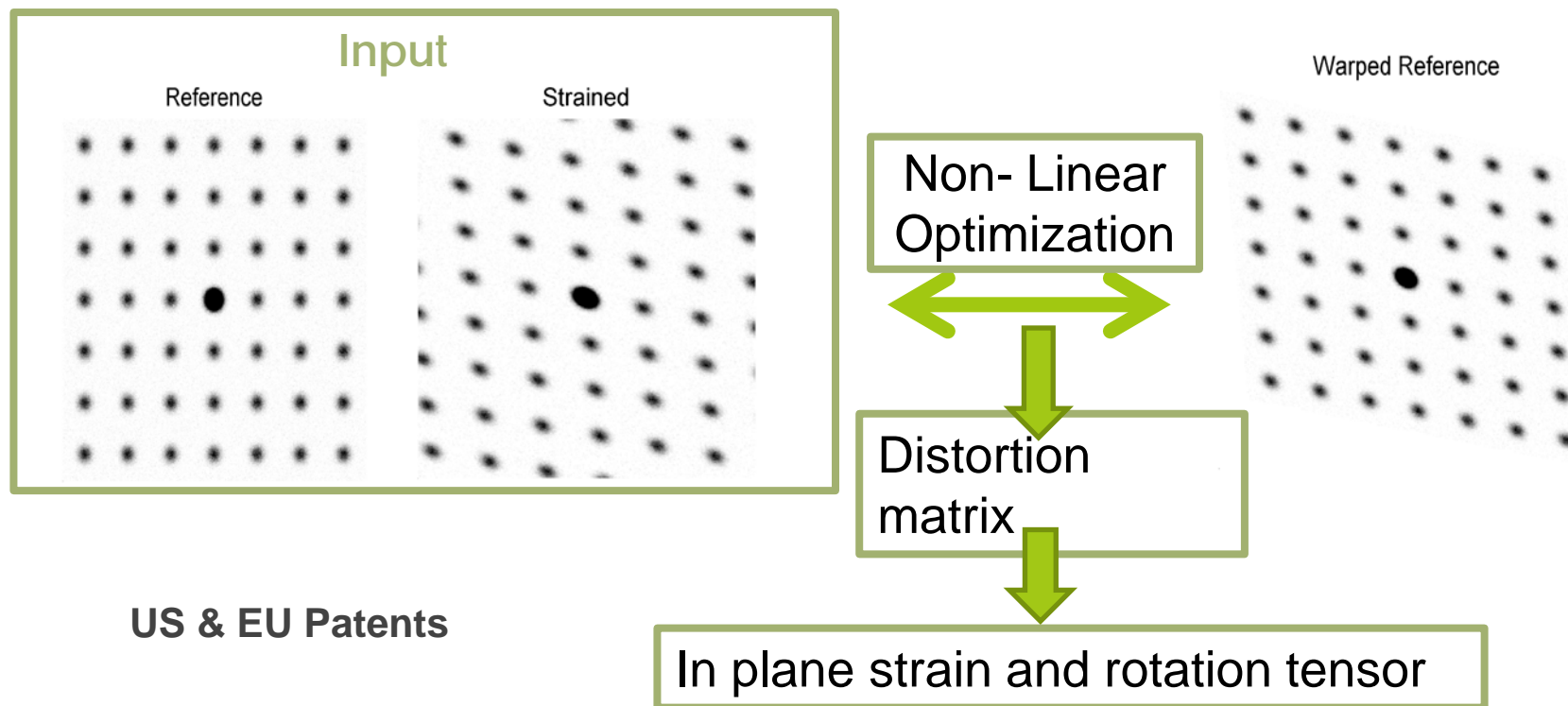
PED is "ideal" (X-Ray like) kinematical pattern
INDEPENDENT of thickness variations !



Vincent-Midgley Precession Method

TOPSPIN Strain Measurement Analysis

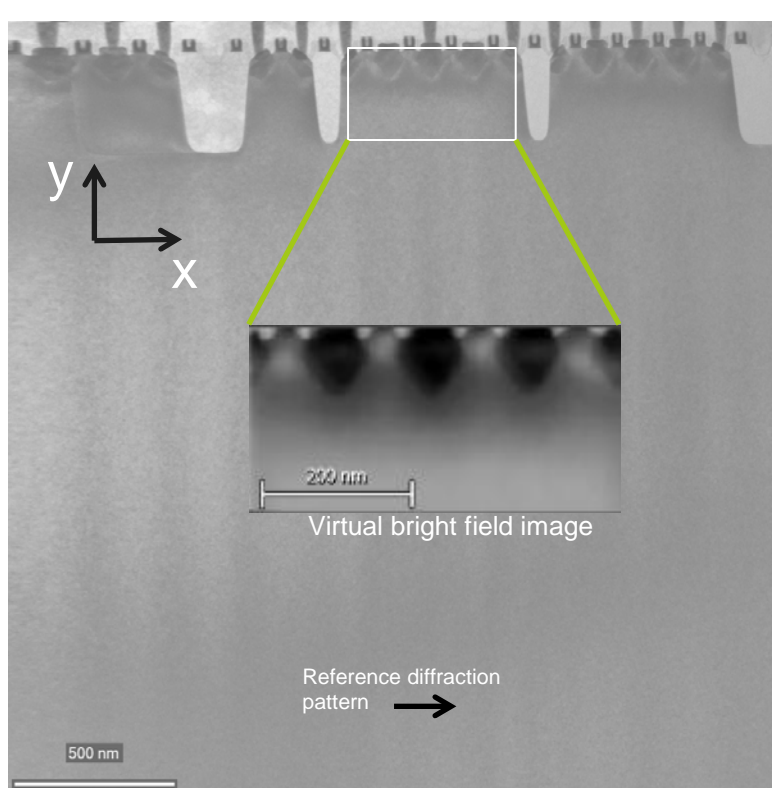
- Diffraction patterns from strained region are matched against a reference pattern
- **All pixels utilized, not just selected spot centers**



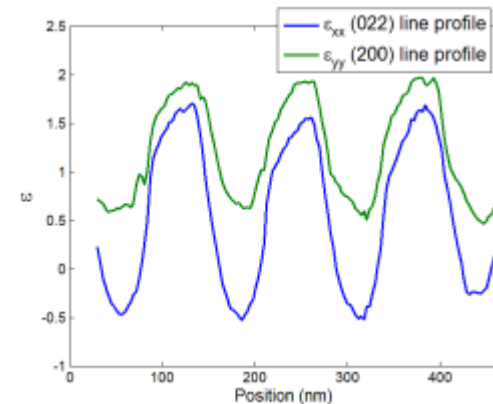
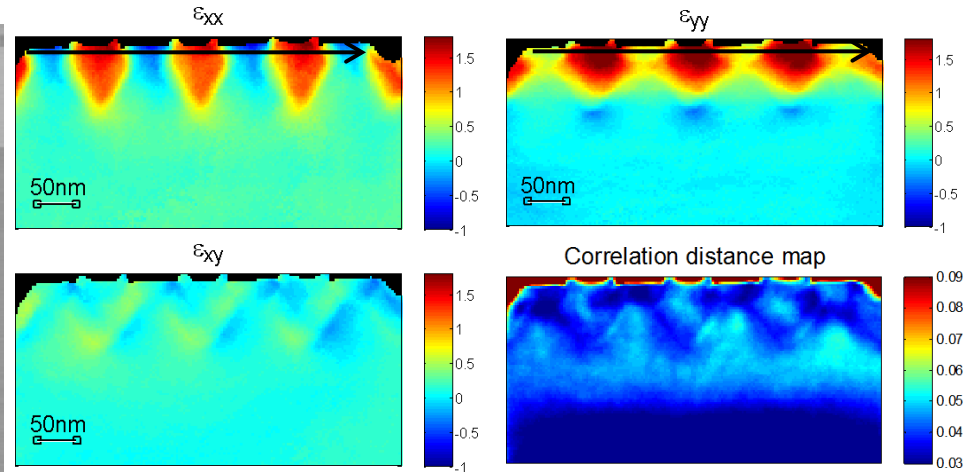
Typical performance of Topspin Strain

- Practical spatial resolution @ 1 degree precession angle : 1 to 5 nm (FEG TEM)
- Sensitivity (precision) @ 1 degree precession angle : 0.1% to 0.01 %
- Spatial resolution and sensitivity depends on model TEM, beam current, beam convergence and sample quality/thickness
- Fast and automated 1D & 2D Strain Mapping at the nanoscale

pMOS Strain Mapping with precession



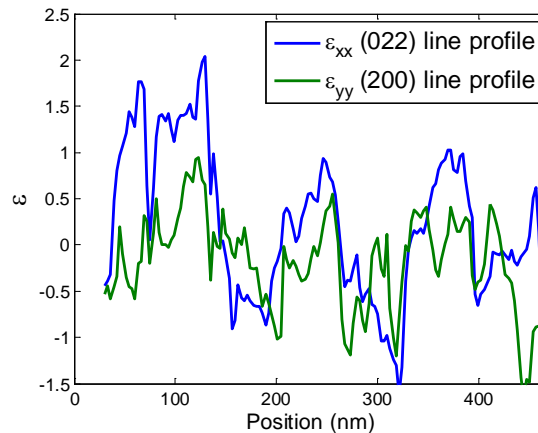
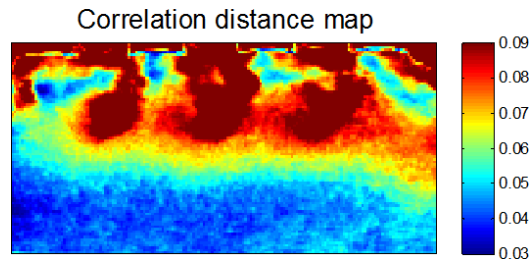
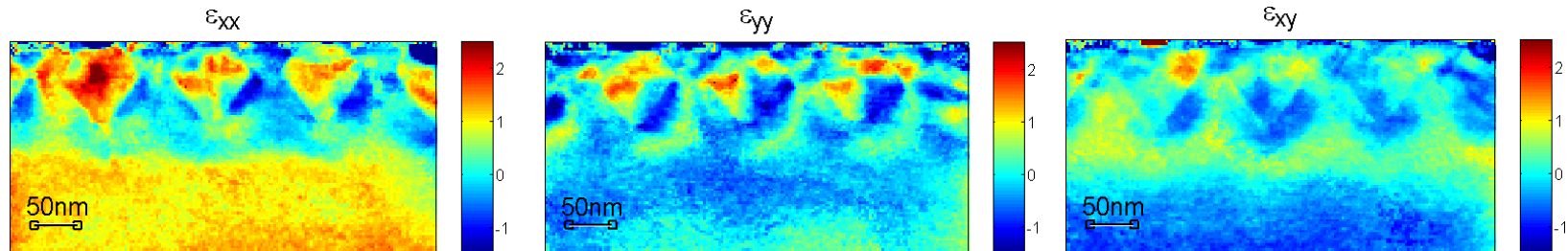
TEM: JEOL ARM200F
Step size: 3 nm
Precession angle: 0.7°



strain values in percent

pMOS Strain Mapping without precession

Same pMOS region without precession

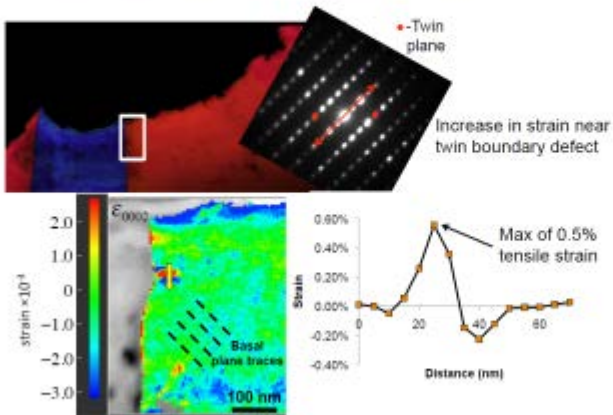


All strain values in percent

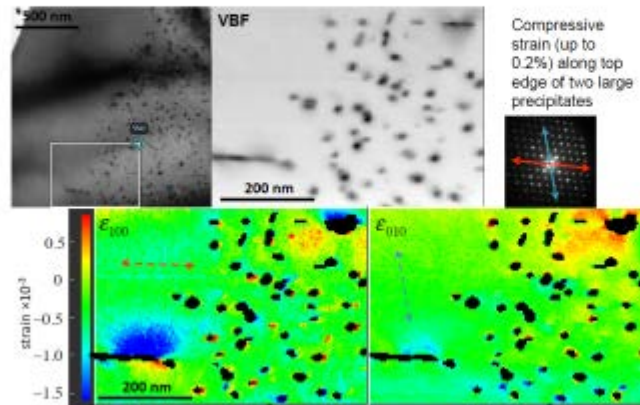
TEM: JEOL ARM200F
Step size: 3 nm
No precession

Strain Mapping in metals

Measuring strain near Mg deformation twins

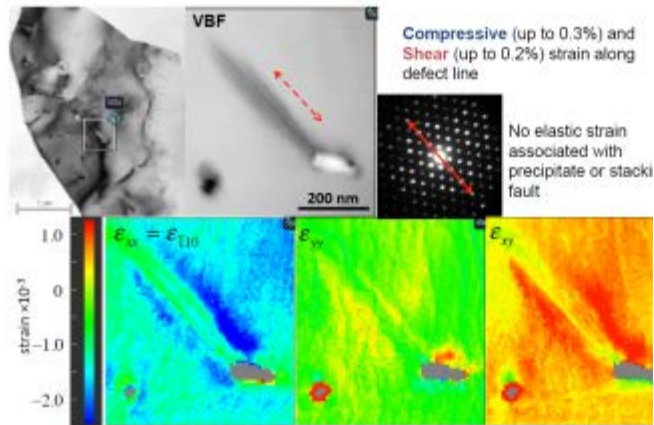


Strain mapping near nanoscale AlN precipitates

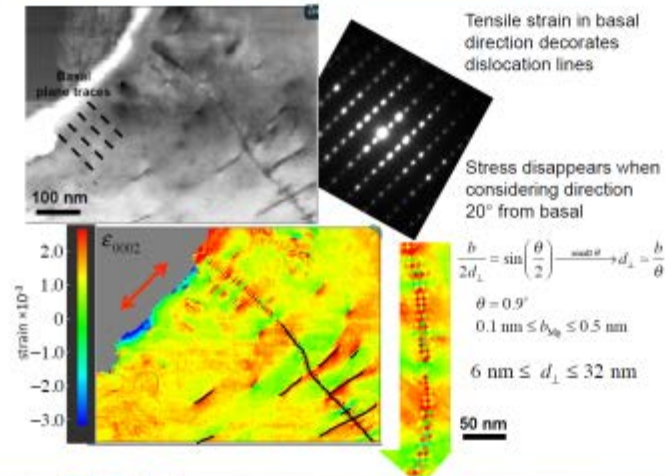


Courtesy Prof. K.Hemker Jons Hopkins University

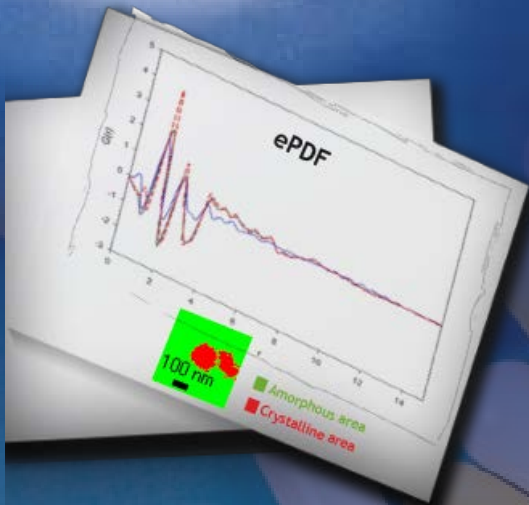
Strain mapping near larger AlN precipitate

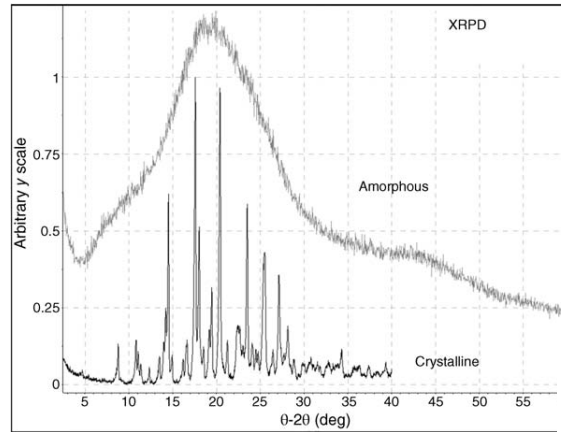
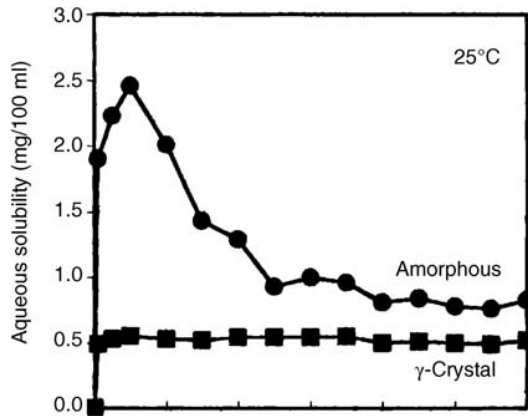


Measuring strain near Mg deformation twins

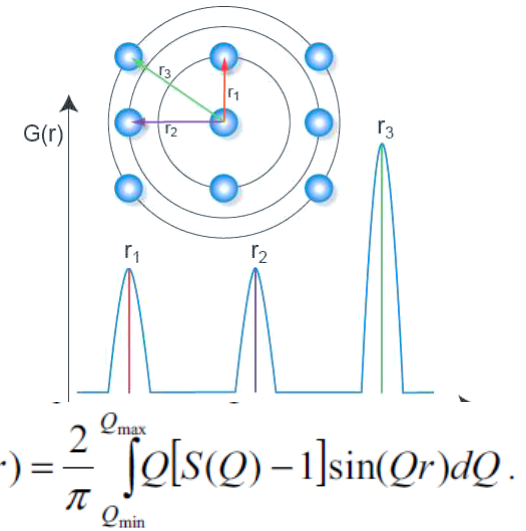


Study Amorphous materials with e-PDF



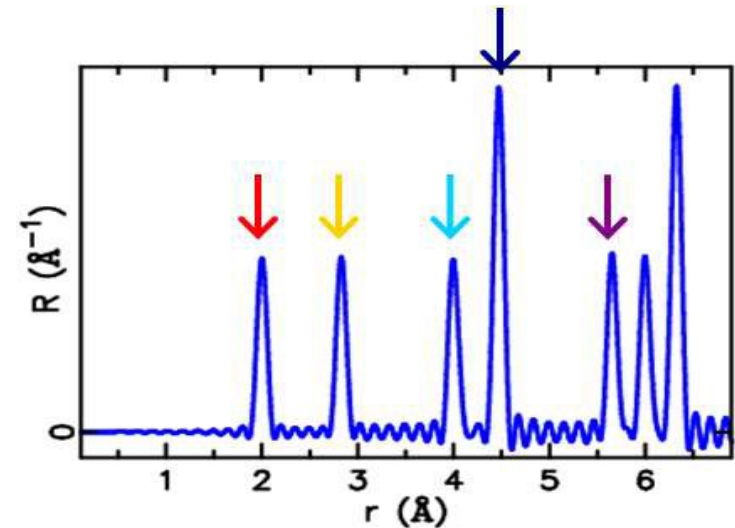
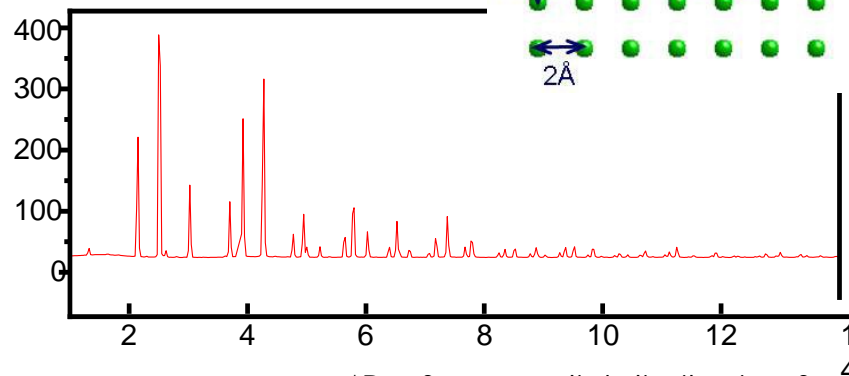
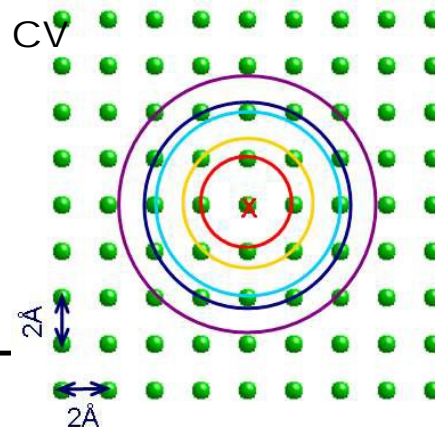
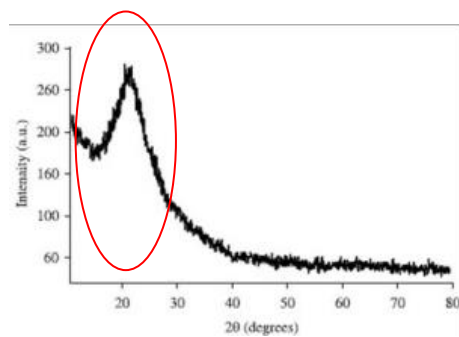


Solubility vs time for crystalline and amorphous indomethacin in water (Book A. Newman Pharmaceutical ASD Wiley 2015)



Amorphous /short range order systems can be described by the Pair Distribution Function (PDF) that provides the probability of finding a distance “r” between two atoms in the material

A total pair-distribution function (PDF) is obtained by repeating this process systematically by placing each atom in the origin.

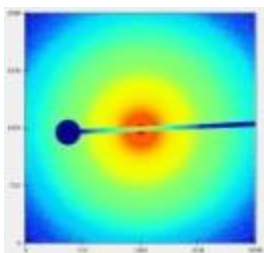


*R refers to radial distribution function

Z. Kristallogr. Supp. 26(2007) 17-26

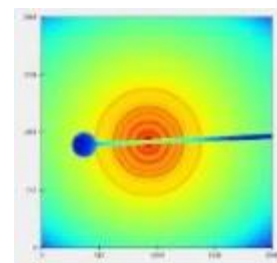
PDF for amorphous and nanomaterials

amorphous

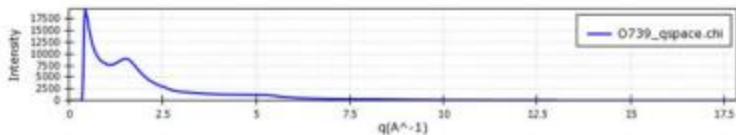


X-Ray diffraction data $I(q)$

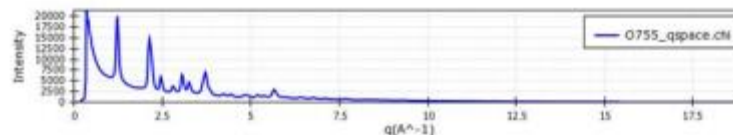
Nanomaterial



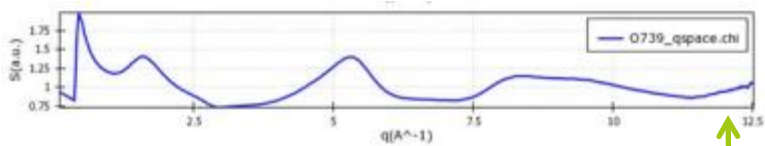
Corrected and Integrated data $I(q)$



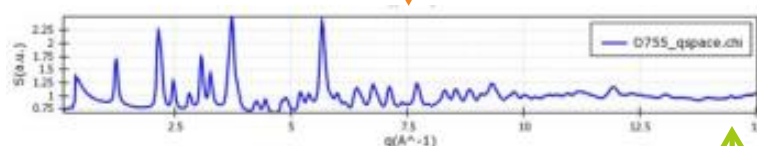
Corrected and Integrated data $I(q)$



Normalization to calculate $S(q)$



Normalization to calculate $S(q)$

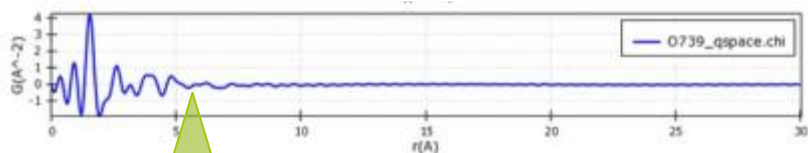


↑ Q_{max} for FT

↑ Q_{max} for FT

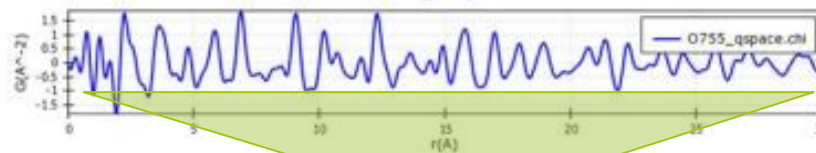
Fourier transformation

PDF

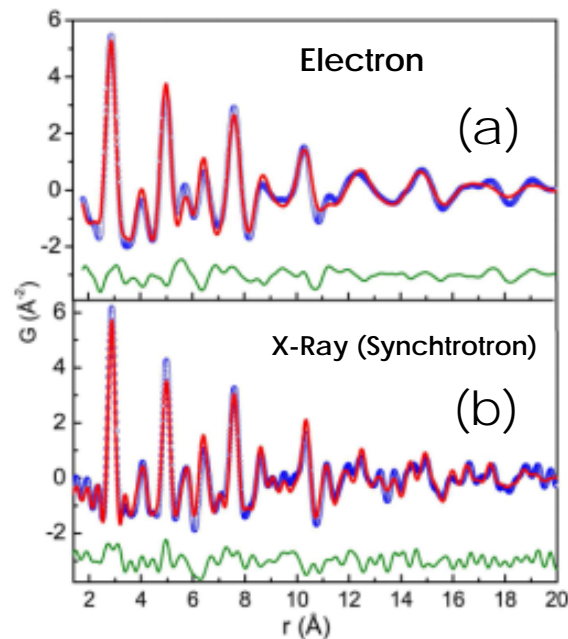
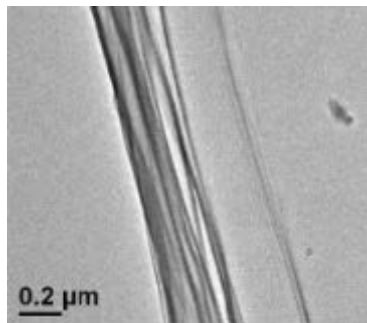


Fourier transformation

PDF



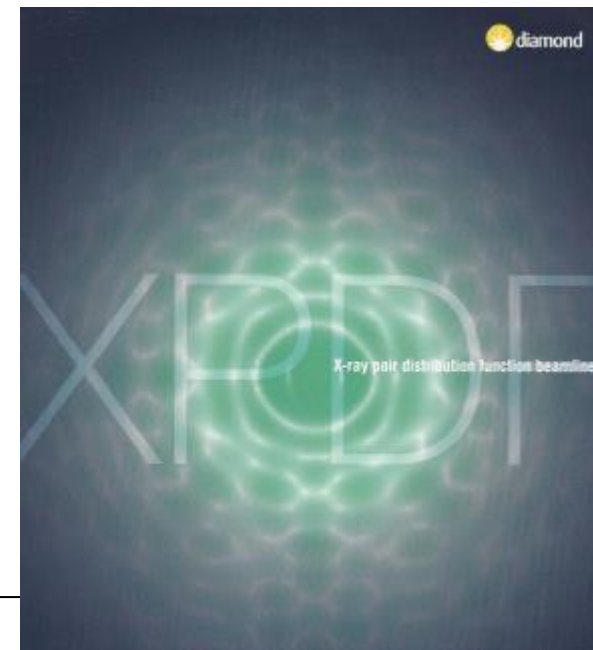
Comparison e- PDF vs Synchrotron X-Ray PDF Au nanoparticles



Fitting of Au structure model
with PDF

- (a) e- PDF calculated from ED Data
- (b) PDF calculated from X-Ray data

PDF obtained from electron diffraction data and PDF obtained from X-ray are fully comparable, using e-PDF very small amorphous areas can be studied

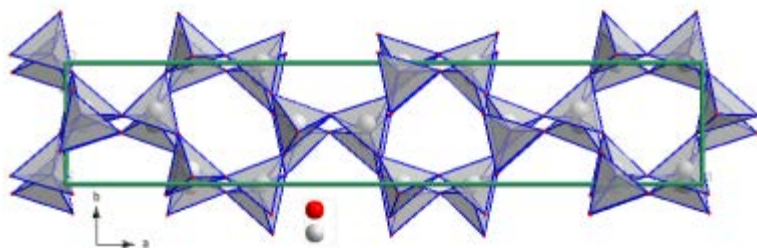


Honduras Opal: Understanding the Local Structure

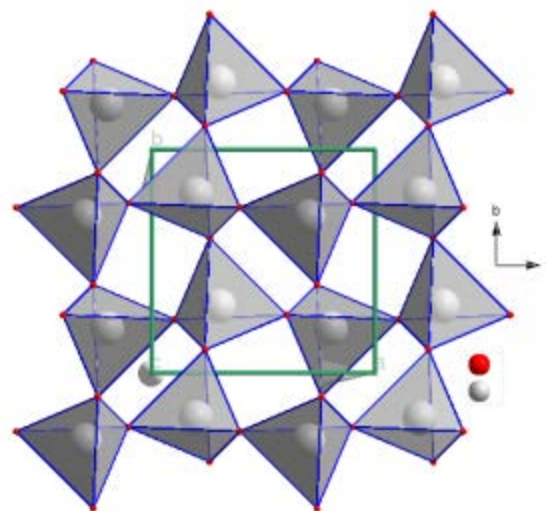
Opal is hydrated silicon dioxide

Can be Microcrystalline, Nano Crystalline or Amorphous

Microcrystalline opal are stacking of cristobalite and tridymite over very short range scale

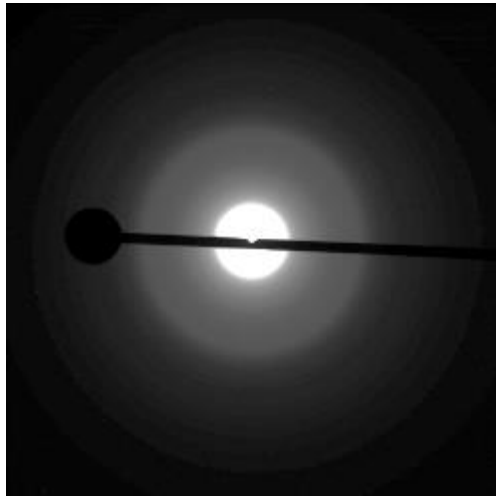


Structure of tridymite



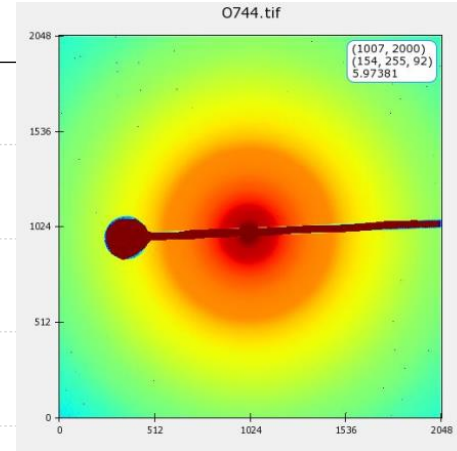
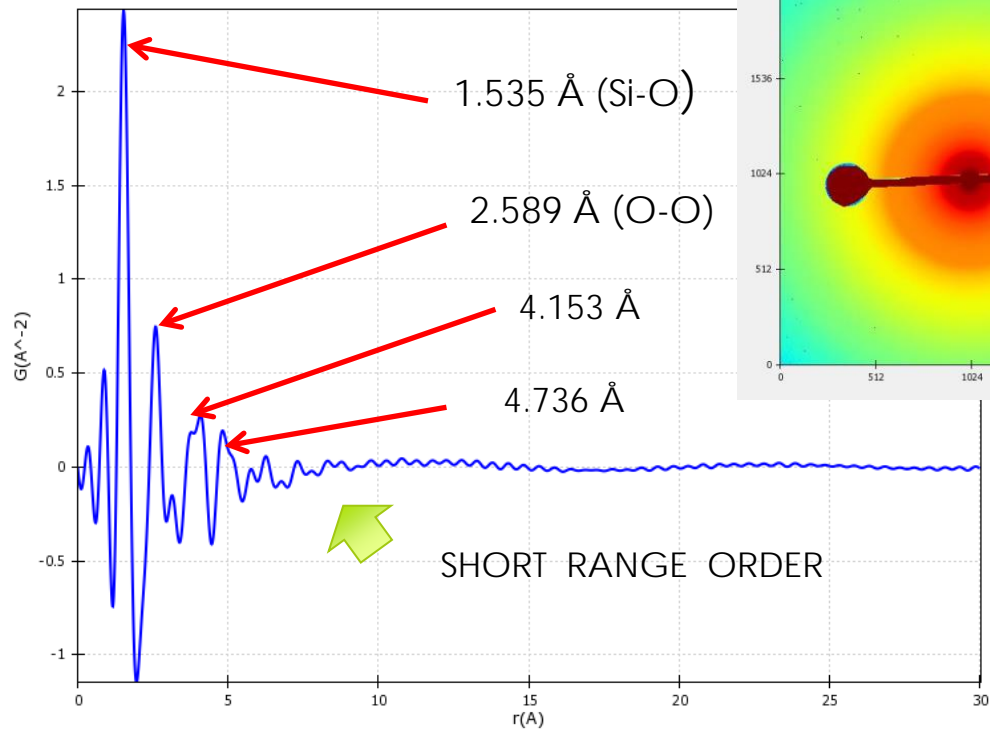
Local Structure of Opal Type C (α -Cristobalite)

Honduras Opal



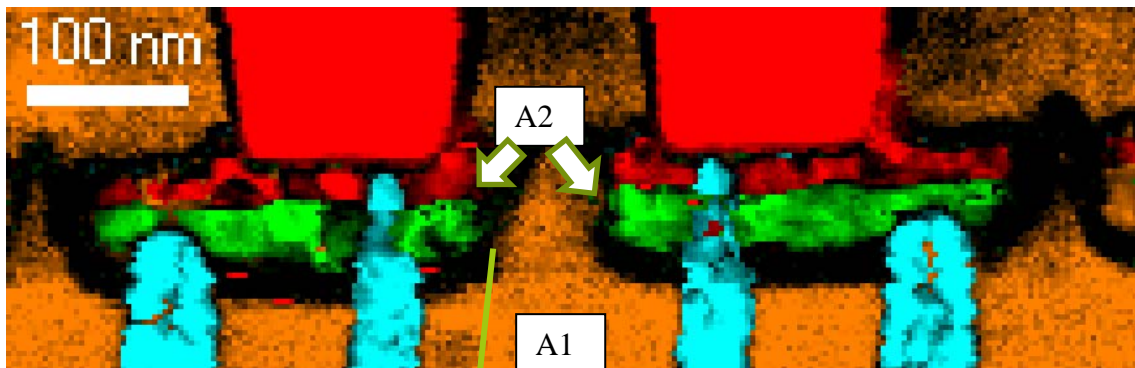
Data Collected on Zeiss 120 KV

Mineral: Cristobalite SiO_2
 $a=7.12 \text{ \AA}$ (cubic)



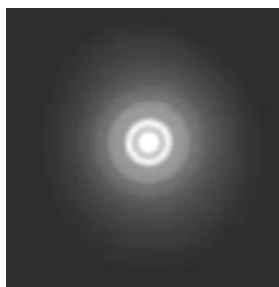
Bond Distances Below 5 Å
 Si - O : 1.5415 Å
 O - O : 2.5173 Å
 Si - Si : 3.0831 Å

e-PDF analysis on amorphous semiconductors



■ Bank_200kV_[Si]_50_0.5_r3.5
■ Bank_200kV_[NiSi_Rabadanov]_100_1_r3.5

■ Bank_200kV_[Tungsten]_100_1_r3.5
■ Bank_200kV_[]_amorphous_1_r1.2

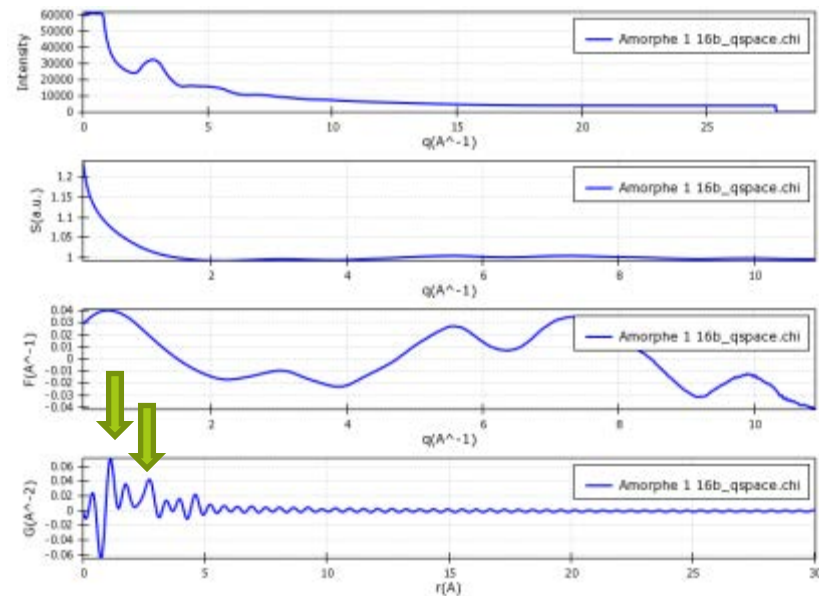


A1 region SiO₂ amorphous
 A2 (black) region Si₃N₄ amorphous

e-PDF analysis on amorphous semiconductors

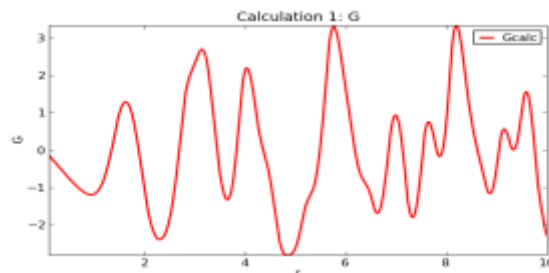


Gatan CCD 2kx 2k Qmax 10 Å⁻¹



Distances found from PDF analysis match Si₃N₄ amorphous

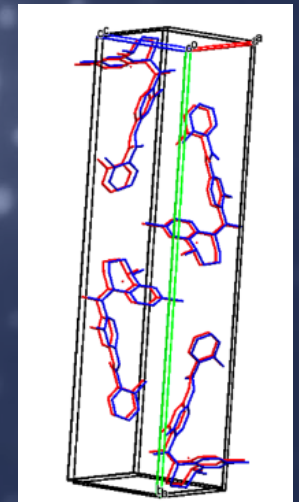
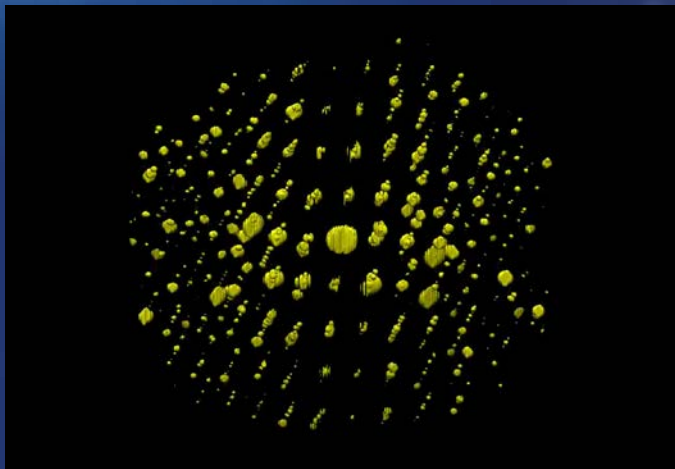
1.10 Å
1.747 Å
2.75 Å



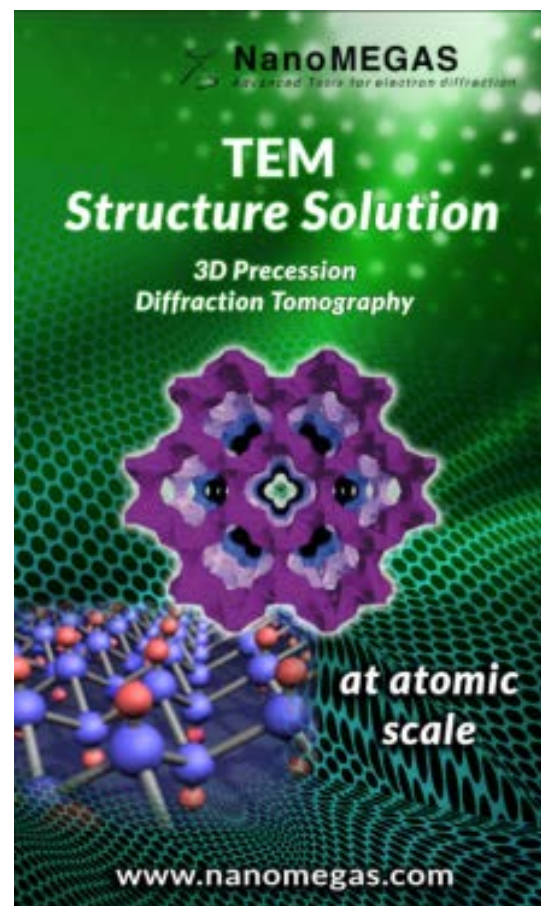
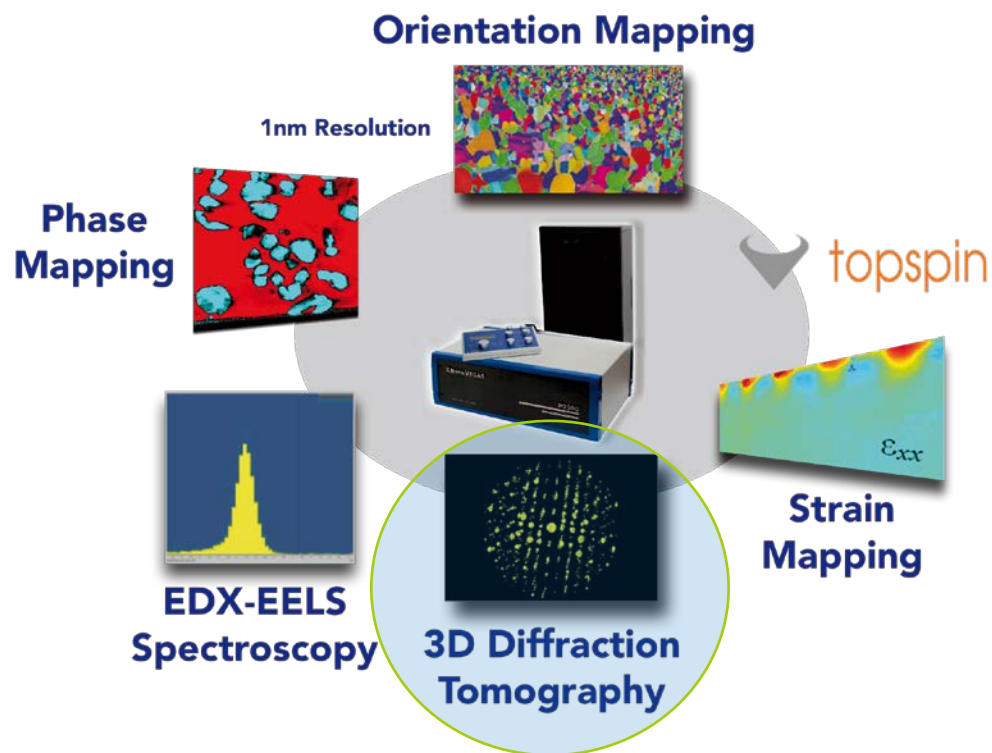
Si₃N₄

Image courtesy E.Rauch and SIMAP
 Grenoble, ST Microelectronics

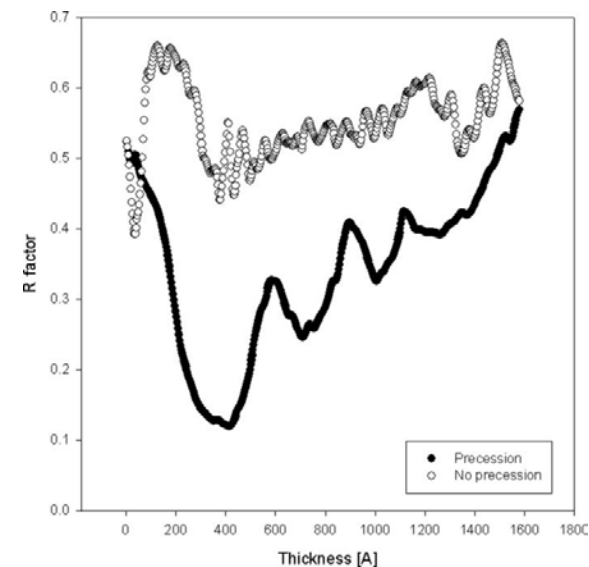
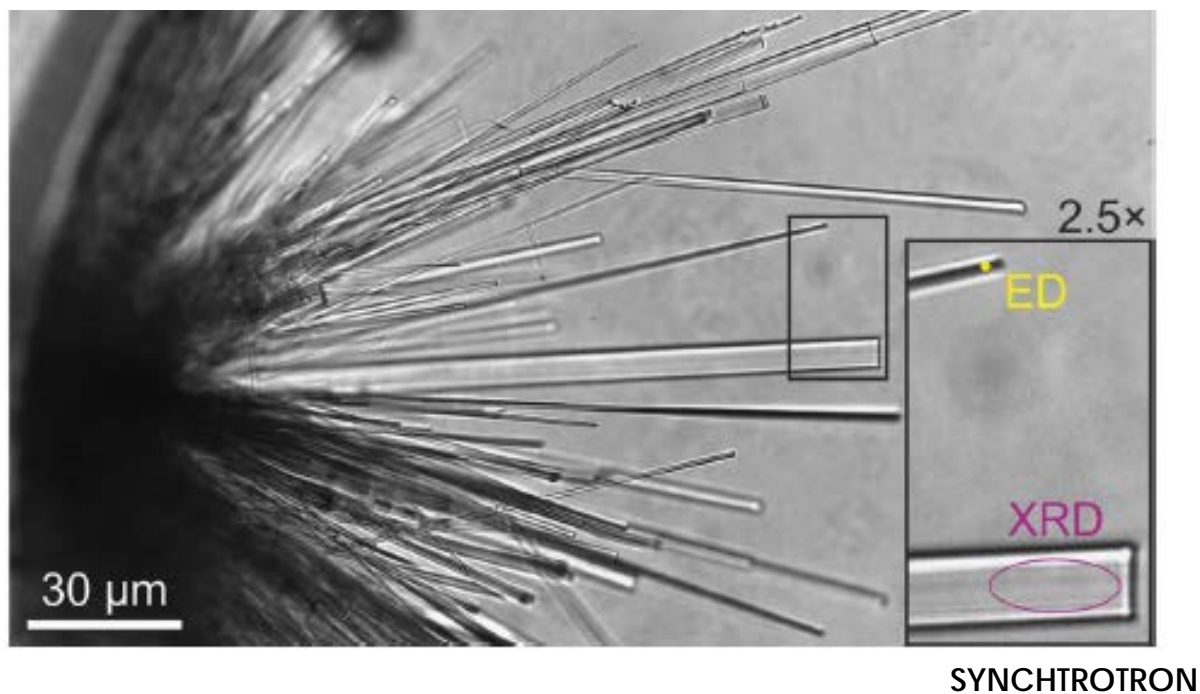
3D Diffraction Tomography



3D Diffraction Tomography TEM Precession Electron Diffraction



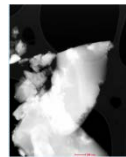
Own et al. (2006), Acta Cryst. A62



**HIGH PRECESSION ANGLE
IMPROVES CRYSTAL STRUCTURE DETERMINATION**

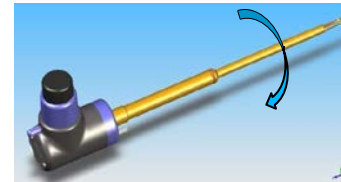
3D Diffraction Tomography

3D TEM diffraction tomography :
3D reconstruction of reciprocal space



500 nm

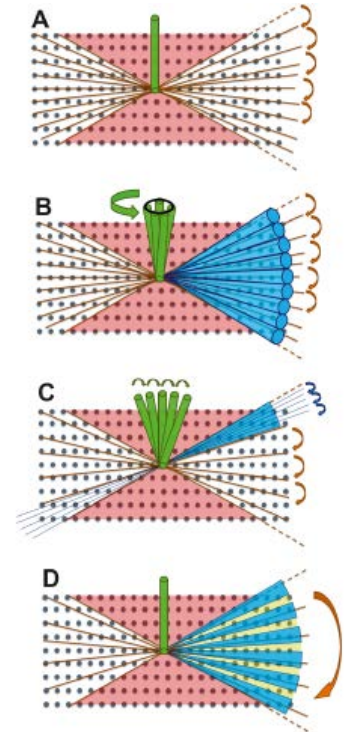
1° Tilt
(total +/- 60°)



Crystal tracking



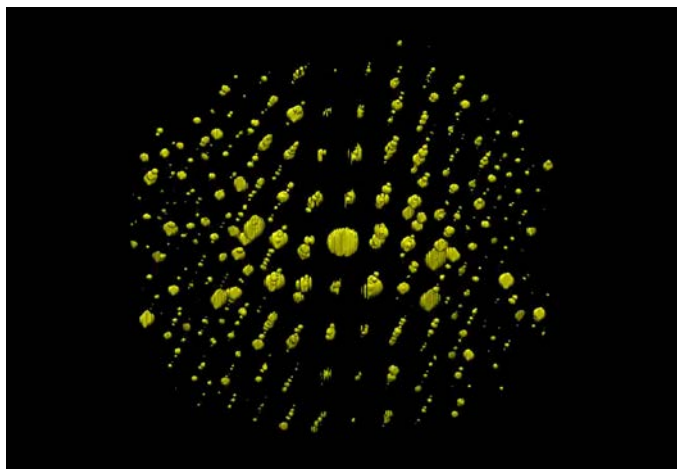
Electron diffraction acquisition



- ✓ complete or almost complete diffraction data to **extract unit cell and crystal symmetry**
- ✓ conceptually simple, data can be taken **with any CCD camera**
- ✓ solution of structures by direct methods or simulated annealing

R close to 15-35 % : reveal all 3D atomic positions with 5-30 pm precision !

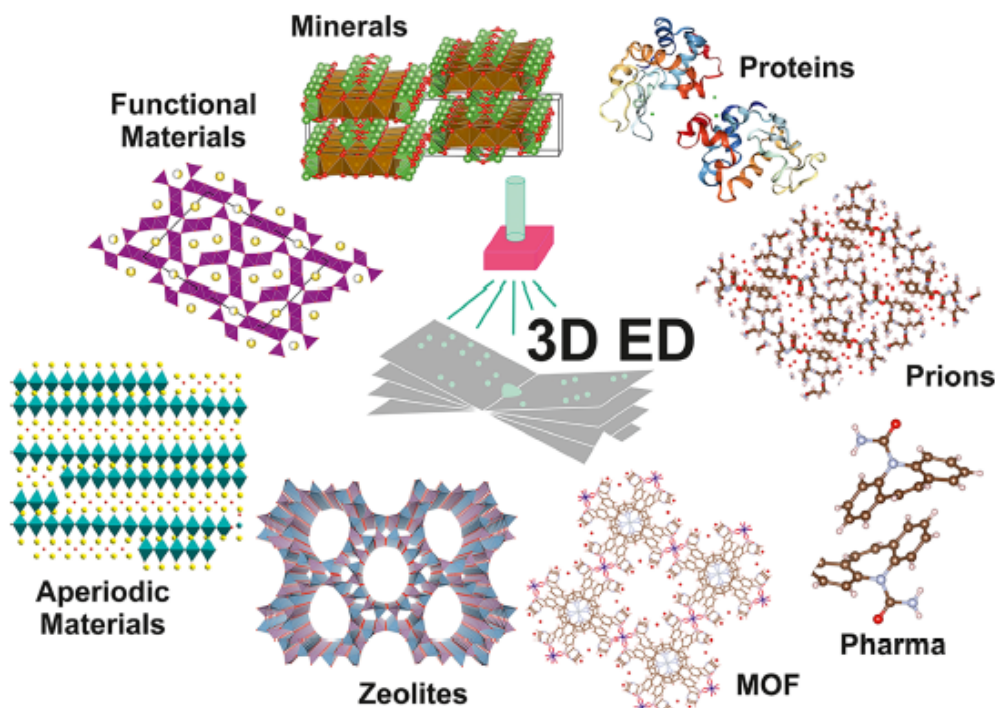
3D TEM Diffraction Tomography for 3D atomic structure solution



Hemimorphite		Reference structure (X-ray and neutron diffraction)			3D precession diffraction Tomography			$\Delta(\text{\AA})$
Atoms	Label	X	Y	Z	X	Y	Z	
Zn	Zn	0.2047(1)	0.1613(1)	0	0.205	0.160	0	0.02
Si	Si	0	0.1465(2)	0.5076(5)	0	0.141	0.529	0.12
O	O1	0.1604(8)	0.2055(1)	0.6363(4)	0.152	0.217	0.657	0.18
O	O2	0	0.1669(2)	0.1938(4)	0	0.156	0.204	0.12
OH	O3	0.3050(2)	0	0.0410(6)	0.289	0	0.073	0.21
O	O4	0	0	0.5912(6)	0	0	0.601	0.05
H ₂ O	O5	1/2	0	0.5195(13)	1/2	0	0.491	0.15
Mayenite		Reference structure			Electron			$\Delta(\text{\AA})$
Atoms	Label	X	Y	Z	X	Y	Z	
Ca	Ca	0.89096(5)	0	3/4	0.902	0	3/4	0.14
Al	Al1	0.01866(3)	0.01866(3)	0.01866(3)	0.018	0.018	0.018	<0.02
Al	Al2	1/4	7/8	0	1/4	7/8	0	-
O	O1	0.18556(3)	0.18556(3)	0.18556(3)	0.184	0.184	0.184	0.03
O	O2	0.44182(4)	0.15035(3)	0.03677(4)	0.439	0.148	0.041	0.06
Y _{0.8} Pr _{0.2} Ba ₂ Cu ₃ O ₇		Reference structure			Electron			$\Delta(\text{\AA})$
Atoms	Label	X	Y	Z	X	Y	Z	
Ba	Ba	0.5	0.5	0.1850(2)	0.5	0.5	0.1874	0.05
Y/Pr	Y	0.5	0.5	0.5	0.5	0.5	0.5	-
Cu	Cu1	0	0	0	0	0	0	-
Cu	Cu2	0	0	0.3565(5)	0	0	0.355	<0.02
O	O1	0	0.5	0	0	0.5	0	-
O	O2	0	0	0.1566(23)	0	0	0.160	<0.02
O	O3	0.5	0	0.3776(21)	0.5	0	0.382	0.06
O	O4	0	0.5	0.3765(21)	0	0.5	0.383	0.06

**Kinematical refinement : Find all 3D atomic positions
with 2-15 pm accuracy !**

> 300 structures solved with ED (2004 - 2019)



3D Electron Diffraction: The Nanocrystallography Revolution

Mauro Gemmi,^{1,†} Enrico Mugnaioli,¹ Tatiana E. Gorelik,² Ute Kolb,^{3,||} Lukas Palatinus,¹ Philippe Boulay,⁴ Sven Hovmöller,⁵ and Jan Pieter Abrahams^{6,†,||}

¹Center for Nanotechnology Innovation@NEST, Istituto Italiano di Tecnologia, Piazza S. Silvestro 12, 56127 Pisa, Italy
²University of Ulm, Central Facility for Electron Microscopy, Electron Microscopy Group of Materials Science (EMMS), Albert Einstein Allee 11, 89081 Ulm, Germany
³Institut für Anorganische Chemie und Analytische Chemie, Johannes Gutenberg-Universität, Duesbergweg 10-14, 55128 Mainz, Germany
⁴Institut für Angewandte Geowissenschaften, Technische Universität Darmstadt, Schnittspahnstraße 9, 64287 Darmstadt, Germany
⁵Department of Structure Analysis, Institute of Physics of the CAS, Na Slovance 2, 182 21 Prague 8, Czechia
⁶CRISMAT, Normandie Université, ENSICAEN, UNICAEN, CNRS UMR 6508, 6 Bd Maréchal Juin, F-14050 Cedex Caen, France
^{||}Inorganic and Structural Chemistry, Department of Materials and Environmental Chemistry, Stockholm University, 106 91 Stockholm, Sweden
[†]Center for Cellular Imaging and NanoAnalytics (C-CINA), Biozentrum, Basel University, Mattenstrasse 26, CH-4058 Basel, Switzerland
[‡]Department of Biology and Chemistry, Paul Scherrer Institut (PSI), CH-5232 Villigen PSI, Switzerland
[§]Leiden Institute of Biology, Leiden University, Sylviusweg 72, 2333 BE Leiden, The Netherlands

ABSTRACT: Crystallography of nanocrystalline materials has witnessed a true revolution in the past 10 years, thanks to the introduction of protocols for 3D acquisition and analysis of electron diffraction data. This method provides single-crystal data of structure solution and refinement quality, allowing the atomic structure determination of those materials that remained hitherto unknown because of their limited crystallinity. Several experimental protocols exist, which share the common idea of sampling a sequence of diffraction patterns while the crystal is tilted around a noncrystallographic axis, namely, the goniometer axis of the transmission electron microscope sample stage. This Outlook reviews most important 3D electron diffraction applications for different kinds of samples and problematics, related with both materials and life sciences. Structure refinement including dynamical scattering is also briefly discussed.

1. INTRODUCTION

Accelerated electrons have been long considered the less promising among the radiation types used in crystallography for attaining diffraction data suitable for atomic structure determination. In fact, the large majority of structural models deposited in crystallographic databases^{1–3} have been obtained by means of X-ray diffraction, and most of what is left has been derived from neutron diffraction or spectroscopic methods. Although still limited, the use of electron diffraction has grown rapidly over the past decade, mostly due to the introduction of 3D methods for the systematic acquisition and analysis of diffracted intensities. Here, we would like to examine how the use of parallel beam electron diffraction for structure determination has evolved from a mostly qualitative technique, used only by few specialists, to a quantitative approach accessible to a much larger community.

To understand the full picture of this (r)evolution, it is important to focus on the strengths of accelerated electrons for

crystallography. First, the possibility to have parallel electron probes with a size of a few nanometers allows collecting diffraction data from sample volumes 2 or 3 orders of magnitude smaller than the ones suitable for synchrotron microfocused X-ray beams. Second, the ability to deliver both diffraction and imaging from the same nanovolume allows the combination of reciprocal and direct space information and the experimental determination of crystallographic phases. Third, the strong Coulomb interaction between electrons and matter allows a good signal-to-noise ratio even from very thin samples and an easier identification of light atoms, like lithium and hydrogen, when compared with X-rays.

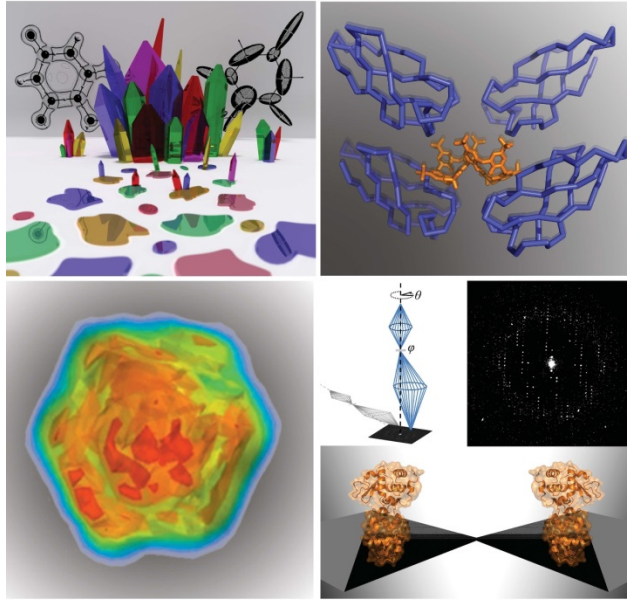
However, the strong scattering of electrons is also the reason why electron diffraction (ED) was disregarded for many years for structure analysis. The occurrence of multiple scattering

Received: April 17, 2019

IUCrJ

www.iucrj.org

Volume 6 | Part 2 | 1 March 2019



ISSN 2052-2525



International Union of
CRYSTALLOGRAPHY

New frontier

Protein 3D Tomography (Micro-ED)

Research papers

IUCrJ
ISSN 2052-2525
CRYO-EM

Received 17 October 2018
Accepted 13 December 2018

Edited by T. Walter, Boston University School of Medicine, USA

Keywords: macromolecular crystallography; electron crystallography; nanobeam precession-assisted electron diffraction; microED; lysozyme; rotation strategy

PMI submission for egg-white lysozyme, X-ray diffraction structure, 3D electron diffraction structure, 4hkl

Supporting information: this article has supporting information at www.iucrj.org

Nanobeam precession-assisted 3D electron diffraction reveals a new polymorph of hen egg-white lysozyme

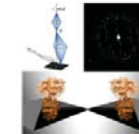
Arianna Lanzi, Eleonora Margheriti, Enrico Mugnaioli, Valentina Cappello, Gianpietro Gazzarè and Mauro Gemmi*

Centre for Nanotechnology Innovation@CNR, Istituto Nazionale di Cristallografia, Piazza San Silvestro 13, 00127 Roma, Italy
*Correspondence e-mail: gianpietro.gazzarè@ic.cnr.it, mauro.gemmi@ic.cnr.it

Recent advances in 3D electron diffraction have allowed the structure determination of several model proteins from submicroscopic crystals, the unit-cell parameters and structures of which could be immediately validated by known models previously obtained by X-ray crystallography. Here, the first new protein structure determined by 3D electron diffraction data is precession-assisted submicroscopic crystals simply by vapor diffusion starting from previously reported crystallization conditions. Remarkably, the data were collected using a low-dose stepwise experimental setup consisting of a precession-oriented nanobeam of ~150 nm, which has never previously been applied for solving protein structures. The crystal structure was additionally validated using X-ray synchrotron radiation sources by both powder diffraction and single-crystal micro-diffraction. 3D electron diffraction can be used for the structural characterization of submicroscopic macromolecular crystals and is able to identify novel protein polymorphs that are hardly visible in conventional X-ray diffraction experiments. Additionally, the analysis which was performed on both nanocrystals and microcrystals from the same crystallization drop suggests that an integrated view from 3D electron diffraction and X-ray microdiffraction can be applied to obtain insights into the molecular dynamics during protein crystal growth.

1. Introduction

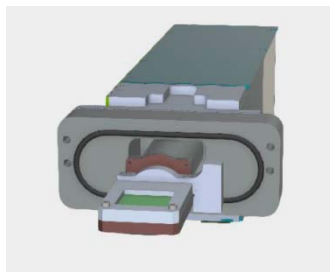
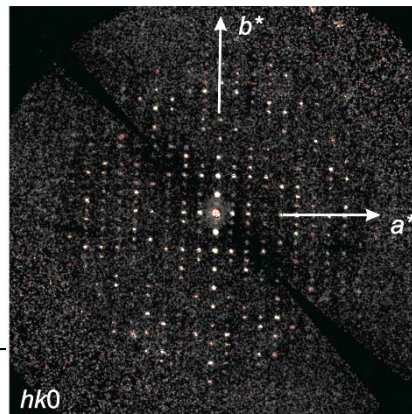
In order to address many challenging scientific issues concerning structural biology, several X-ray microfocus beamlines worldwide are fully dedicated to the analysis of 3D protein crystals smaller than a few tens of micrometres (Smith *et al.*, 2012). The relevance of nanocrystallography is driving some beamlines to achieve beam sizes below 1 µm in order to investigate even smaller protein crystals (Machuga *et al.*, 2016; Owen *et al.*, 2016). However, access for the scientific community to X-ray microfocus beamlines or to unconventional approaches such as X-ray free-electron lasers (XFEL; McNeil & Thompson, 2010) is strongly limited (Giles *et al.*, 2018), and therefore there is growing interest in the development of alternative approaches. In this regard, electron-microscopy methods appear to be particularly promising. Cryo-EM imaging has rapidly become a widespread technique that is able to skip the crystallization step by directly imaging macromolecular complexes or potentially even single molecules of sufficient size (Amunts *et al.*, 2014; Kuhlbrandt, 2014; Cheng, 2015; Nogales & Scheres, 2015; Fernandez-Leiro & Scheres, 2016; Quirinii & Baumeister, 2016).



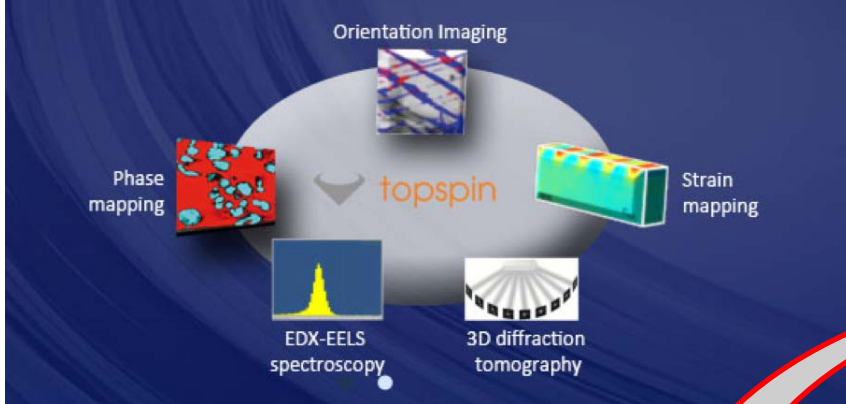
OPEN ACCESS

178 <https://doi.org/10.1107/S2052252518017657>

RUCI (2019), 6, 178–188



Precession Diffraction Solutions

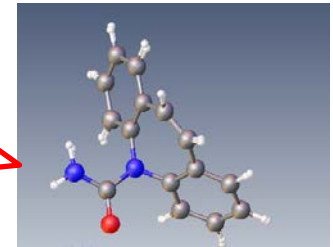


Accurate orientation/phase maps

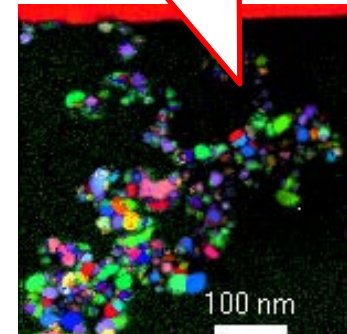
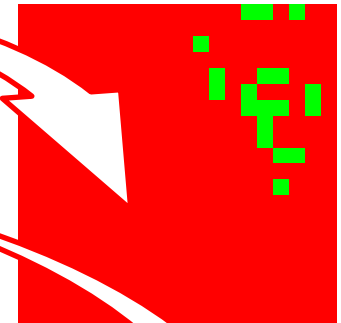
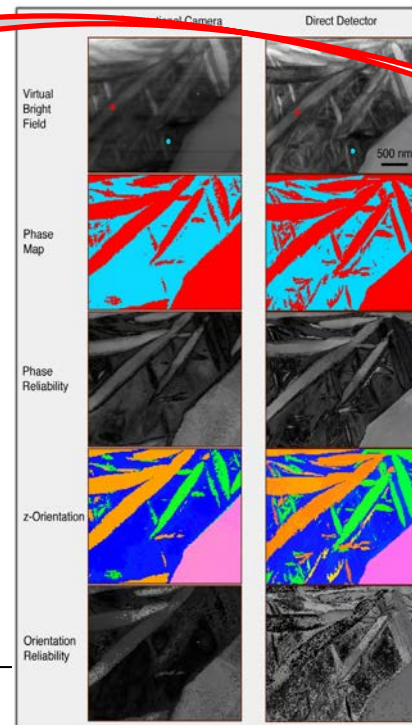
More accurate structures with ED

Low dose sensitive materials

Dynamic phenomena in LC



New fronteers





COWORKERS

Daniel Bultreys (NM)

Joaquim Portillo (NM)

Partha Das (NM)

Alex Gomez (NM)

Thanos Galanis (NM)

Alan Robins (NM)

Muriel Veron (CNRS Grenoble)

Edgar Rauch (CNRS Grenoble)



Merci pour votre attention !

ELECTRON OPTICS
éloïse
INSTRUMENT SERVICE